

The University of Maine
DigitalCommons@UMaine

Electronic Theses and Dissertations

Fogler Library


Spring 5-10-2019

Living on the edge: thermophysiology of the southern flying squirrel at its northern range margin

Vanessa R. Hensley

University of Maine, vanessa.hensley@maine.edu

Follow this and additional works at: <https://digitalcommons.library.umaine.edu/etd>

 Part of the [Comparative and Evolutionary Physiology Commons](#), and the [Other Ecology and Evolutionary Biology Commons](#)

Recommended Citation

Hensley, Vanessa R., "Living on the edge: thermophysiology of the southern flying squirrel at its northern range margin" (2019).
Electronic Theses and Dissertations. 2951.
<https://digitalcommons.library.umaine.edu/etd/2951>

This Open-Access Thesis is brought to you for free and open access by DigitalCommons@UMaine. It has been accepted for inclusion in Electronic Theses and Dissertations by an authorized administrator of DigitalCommons@UMaine. For more information, please contact um.library.technical.services@maine.edu.

**LIVING ON THE EDGE: THERMOPHYSIOLOGY OF THE SOUTHERN FLYING SQUIRREL
AT ITS NORTHERN RANGE MARGIN**

By

Vanessa Hensley

B.A. Washington University in St. Louis, 2013

A Thesis

Submitted in Partial Fulfillment of the

Requirements for the Degree of

Master of Science

(in Ecology and Environmental Sciences)

The Graduate School

The University of Maine

May 2019

Advisory Committee:

Danielle L. Levesque, Assistant Professor of Mammalogy and Mammalian Health, Advisor

Rebecca Holberton, Professor of Avian Biology

Malcolm L. Hunter, Jr., Professor of Wildlife Ecology

**LIVING ON THE EDGE: THERMOPHYSIOLOGY OF THE SOUTHERN FLYING SQUIRREL
AT ITS NORTHERN RANGE MARGIN**

By Vanessa Hensley

Thesis Advisor: Dr. Danielle L. Levesque

An Abstract of the Thesis Presented
in Partial Fulfillment of the Requirements for the
Degree of Master of Science
(in Ecology and Environmental Sciences)
May 2019

Climate change has the potential to upset entire ecological systems, making predictive models of the utmost importance. The incorporation of physiological parameters into predictive models not only bolsters their accuracy but also provides a mechanistic explanation for ecological changes already observed and those yet to come. North American flying squirrels, for example, have already experienced dramatic range shifts northward over recent decades, with climate change being the suspected driver. While other studies have focused on warming winter temperatures, I explored the hypothesis that rising summer temperatures were driving the observed range shifts. Unable to find a reliable population of the northern species, *Glaucomys sabrinus*, I focused on southern flying squirrels, *Glaucomys volans*, to determine the effect of high temperatures on thermoregulation and energy usage. Using flow-through respirometry, I measured the relationship between temperature and metabolic rate/evaporative water loss/body temperature. I used temperature-sensitive data loggers to measure core body temperature in free-ranging flying squirrels to explore an additional thermoregulatory strategy – heterothermy. I discovered no significant increase in metabolic rate in temperatures up to 40°C but did detect an increase in evaporative water loss starting at 36.2°C. Body temperature (T_b) of flying squirrels followed a circadian pattern with ~2°C difference between active and resting phase modal T_b . This daily level of heterothermy is consistent with, but slightly higher, than other squirrel species according to the Heterothermy Index. High temperatures are unlikely to cause an energetic strain on southern flying squirrels in Maine as long as water resources remain available. Measurements of microclimate, accounting for group nesting and cavity insulation, are still needed to fully understand the extent of heterothermy and the influence of high ambient temperature on the thermoregulation of *G. volans* in Maine.

DEDICATION

This thesis is dedicated to my father, Larry Hensley. You have been unrelenting in the pursuit of education and knowledge in your own life and have encouraged me to do the same. You continually push me to do more and be more than I think possible, and for that, I am forever grateful.

ACKNOWLEDGMENTS

The biggest thank you goes to my dedicated advisor, Dr. Danielle L. Levesque. Her guidance and support throughout every aspect of this project was unparalleled, and I am honored to be her first graduate student. Thank you to my committee members Dr. Rebecca Holberton and Dr. Malcolm Hunter Jr. for your flexibility and thought-provoking advice. This work could not have been completed without the help of reliable and talented field assistants. Thank you to Michelle Bassis, Evalyn Machia, and Tashawna Spellen for bearing with me as I learned the ropes of small mammal handling and respirometry. Thank you to Jake Gutkes and Tal Kleinhouse for your unwavering support and infectious enthusiasm. Thank you to my friends at the University of Maine, Anna McGinn, Will Kochtitzky, Isaac Shepard, and Zach Wood, for helping in every way they could – from extra field assistants to sounding boards to statistics tutors. Lastly, thank you to my family and to Andy Bezek for the motivation and support needed to achieve my goals. Funding for this research was provided by the USDA National Institute of Food and Agriculture, Hatch Project Number 21623 through the Maine Agricultural & Forest Experiment Station and the University of Maine's start-up funds provided to Dr. Danielle L. Levesque. Notable contributions from the University of Maine Graduate School Government and the University of Maine Center for Undergraduate Research supplemented the funding.

TABLE OF CONTENTS

DEDICATION.....	iii
ACKNOWLEDGMENTS.....	iv
LIST OF TABLES.....	vii
LIST OF FIGURES.....	viii
GLOSSARY.....	ix
CHAPTER 1 GENERAL INTRODUCTION.....	1
1.1 Climate Background.....	1
1.2 An Overview of Thermal Physiology.....	3
1.3 Rationale and Objectives.....	6
CHAPTER 2 STUDY SYSTEM – FLYING SQUIRRELS OF MAINE.....	8
2.1 Introduction.....	8
2.1.1 Species Description.....	8
2.1.2 Shifting Ranges.....	11
2.2 Methods.....	14
2.2.1 Capture and Processing.....	14
2.3 Results.....	15
2.4 Discussion.....	16
CHAPTER 3 THERMOPHYSIOLOGY OF SOUTHERN FLYING SQUIRRELS.....	19
3.1 Introduction.....	19
3.2 Methods.....	20
3.2.1 Respirometry.....	20
3.2.1.1 Animal Handling.....	20
3.2.1.2 Flow-Through Respirometry Set-Up.....	21
3.2.1.3 Experimental Protocol.....	23
3.2.1.4 Data Analysis.....	24
3.2.2 Core Body Temperature.....	28
3.2.2.1 Animal Handling.....	28
3.2.2.2 Surgical Implantation.....	28

3.2.2.3 Forest Temperature.....	30
3.2.2.4 Data Analysis.....	30
3.3 Results.....	31
3.3.1 Resting Metabolic Rate.....	31
3.3.2 Core Body Temperature.....	34
3.4 Discussion.....	38
3.5 Conclusions.....	44
REFERENCES.....	46
APPENDIX 1.....	52
APPENDIX 2.....	56
APPENDIX 3.....	57
BIBLIOGRAPHY OF THE AUTHOR.....	58

LIST OF TABLES

Table 1: Southern flying squirrels used for respirometry experiments.....	31
Table 2: Southern flying squirrels used for core body temperature experiments.....	35
Table 3: Heterothermy Index for <i>G. volans</i> individuals.....	37
Table 4: Morphometric measurements for captured <i>G. volans</i> from 2017-2018.....	53
Table 5: Respirometry models.....	56
Table 6: Core body temperature models.....	57

LIST OF FIGURES

Figure 1: Depiction of a Scholander-Irving Curve.....	5
Figure 2: Distribution of <i>G. sabrinus</i> and <i>G. volans</i> in North America.....	9
Figure 3: <i>Glaucomys volans</i> in metabolic chamber used for respirometry experiments.....	21
Figure 4: Chamber temperature over the course of an experiment.....	24
Figure 5: Physiological parameters of <i>G. volans</i> exposed to various ambient temperatures.. ..	34
Figure 6: Core body and ambient temperature traces.....	36
Figure 7: Excerpt of core body temperature trace.. ..	36
Figure 8: Histogram of core body temperature for all implanted <i>G. volans</i>	37
Figure 9: Body Condition Index (BCI) for <i>G. volans</i> from 2017-2018.....	52

GLOSSARY

Basal metabolic rate (BMR) – the minimum sustained rate of energy turnover of an endotherm; animal must be inactive, post-absorptive, adult, nonreproductive, and thermoregulating in their inactive circadian phase (White and Seymour, 2004; Mitchell et al., 2018)

Ectotherm – an animal whose body temperature is determined primarily by passive heat exchange with its environment (Withers, 1992)

Endotherm – an animal whose body temperature is substantially elevated above the ambient temperature by internal, metabolic heat production (Withers, 1992)

Heterotherm – an endotherm that allows its core body temperature to vary based on ambient conditions

Homeotherm – an endotherm that precisely defends a core body temperature despite large variations in ambient temperature

Lower critical temperature (LCT) of the thermoneutral zone – the temperature at which metabolic rate rises above basal level for thermoregulatory purposes (Mitchell et al., 2018)

Respiratory quotient – the ratio of carbon dioxide produced to oxygen consumed through cellular metabolism; indicates the metabolic substrate used (1 for carbohydrate metabolism, 0.7 for lipids, and 0.84 for proteins) (Withers, 1992)

Resting metabolic rate (RMR) – similar to BMR but with less stringent conditions; animals are only required to be resting (Withers, 1992)

Thermoneutral zone (TNZ) – the range of air temperatures over which an endotherm maintains its basal metabolic rate (Withers, 1992)

Torpor – a physiological state of endotherms with a circadian or short-term cycle of lowered body temperature and depressed metabolic rate (Withers, 1992)

Upper critical temperature (UCT) of the thermoneutral zone – the temperature at which metabolic rate rises above basal level (Withers, 1992); the temperature at which evaporative cooling starts (Mitchell et al., 2018)

CHAPTER 1

GENERAL INTRODUCTION

1.1 Climate Background

According to the Intergovernmental Panel on Climate Change, current “global climate warming is unequivocal and unprecedented over decades to millennia” (IPCC, 2014). Each of the last three decades has been successively warmer than any preceding decade since 1850 (IPCC, 2014). Scientists and conservationists alike question the effects global warming will have on ecological systems and individual species, especially if little is done to curb its drivers (Parmesan, 2006). Changes to phenology, migration patterns, ranges, and life history traits have already been observed in both tropical and polar species (Parmesan, 2006). The state of Maine, uniquely positioned in the US, contains three distinct climate zones all anticipated to react differently to global warming (Fernandez et al., 2015). Maine is expected to see higher average temperatures due to the lengthening of summer and the increased incidence of high heat days (Fernandez et al., 2015).

How global warming will affect whole ecosystems as well as individual species has become a major avenue of research in biology and ecology. One commonly used method for predicting future changes is a bioclimatic envelop model. Bioclimatic envelope models use “associations between aspects of climate and known occurrences of species across landscapes of interest to define sets of conditions under which species are likely to maintain viable populations” (Araujo and Peterson, 2012). Defined sets of conditions are mapped to future climate projections and predictions of species’ ranges and prevalence emerge. Bioclimatic envelope models are simplistic in their requirements and application and are often criticized for

just that reason (Araujo and Peterson, 2012; Kearney et al., 2009). The models focus solely on abiotic factors as predictor variables. Though undeniably important, abiotic factors are not the only factors affecting a species' success in the face of climate change (Araujo and Peterson, 2012; Kearney et al., 2009; Parmesan, 2006). Biotic factors such as mutualistic relationships, predator-prey dynamics, and interspecific competition play a vital role in determining the range and success/vitality of a given species (Sexton et al., 2009). Furthermore, because bioclimatic envelope models rely on current associations between species and variables, there is no room to predict what will occur under novel conditions. Climate change will undoubtedly introduce new conditions as communities shift and ecosystems change, forcing species to exploit new biotic and abiotic opportunities and limitations that may not have previously existed (Hobbs et al., 2009).

Another component lacking in bioclimatic envelope models is any consideration of physiology (Huey et al., 2010; McCain and King, 2014; Mitchell et al., 2018). Current associations between individual species and abiotic conditions allude to the absolute limits of physiology but do not encompass them. A species may be living at the extremes of its physiological tolerance or safely in the middle, a detail not evident in current range distributions. Physiological research is recognizably tedious and not easily performed at large scales, especially for mammals, but that does not negate its importance (McCain and King, 2014). Physiology provides a mechanistic explanation for responses that are only hypothesized using simple bioclimatic envelope models (Seebacher and Franklin, 2012).

The first step in building physiologically-inclined models is collecting the necessary data. As evidenced by Huey et al. (2012), this data does exist for a variety of ectotherms and is starting to be incorporated into predictive models. However, little research has focused on the physiological effects of high temperatures on endotherms. Endotherms are inherently difficult to

study because of the complex relationship between environmental temperature and body temperature (Scholander, 1955; Porter and Gates, 1969). While ectotherm body temperature varies directly and in close synchrony with environmental conditions, endotherms are able to buffer the effects of environmental variation in order to maintain an elevated body temperature (Scholander, 1955; Porter and Gates, 1969). The few endothermic species that have been extensively studied primarily reside in polar regions, where temperatures are expected to increase most dramatically, or exhibit extreme thermal adaptations such as hibernation or torpor (Chappell and Bartholomew, 1981; Humphries, 2004). Nevertheless, temperate and tropical species will face their own set of challenges. Temperate species already experience a variable climate and, along with hotter temperatures, are predicted to experience even more variability as climate change progresses (Parmesan, 2006; IPCC, 2014). With so many species residing in the temperate zone, physiology-informed predictive models are crucial to conservation in this area of the world.

1.2 An Overview of Thermal Physiology

The field of thermal physiology employs many techniques to understand the relationship between temperature and physiology. Flow-through respirometry is one such technique that focuses on the relationship between temperature and metabolic rate. Respirometry consists of measuring oxygen and/or carbon dioxide levels in expired air to quantify the amount of chemical energy being used by an organism – its metabolic rate (Lighton, 2008). Conducting respirometry experiments under various conditions – high activity, low temperature, growth, etc. – generates energy usage data that can be used to make inferences about survival, behavior, and ecology in the wild.

Energy is used for every aspect of an organism's life from mating to foraging to simply existing (Lighton, 2008; Withers et al., 2016). Endotherms devote a large portion of their energy production to the maintenance of a high, sustained body temperature (Withers, 1992; Ruben, 1995; Withers et al., 2016). However, the amount of energy they are required to dedicate is based on ambient temperature (Withers, 1992; Ruben, 1995). One of the ways we can measure this relationship in resting animals is by determining the parameters of the thermoneutral zone. The thermoneutral zone (TNZ) refers to the range of ambient temperatures in which an endotherm can maintain its desired body temperature through minimal energy expenditure or at a basal metabolic rate (Withers et al., 2016). As temperatures exceed this zone, an endotherm must allocate energy to evaporative cooling or thermogenesis in order to maintain a preferred body temperature (Withers et al., 2016). The limits of the TNZ are referred to as the upper (UCT) and lower critical temperature (LCT). The UCT, LCT, and breadth of the TNZ are species specific and even vary individually to some extent. A graph of the relationship between ambient temperature and metabolic rate in endotherms is referred to as a Scholander-Irving Curve (Figure 1; Scholander et al., 1950).

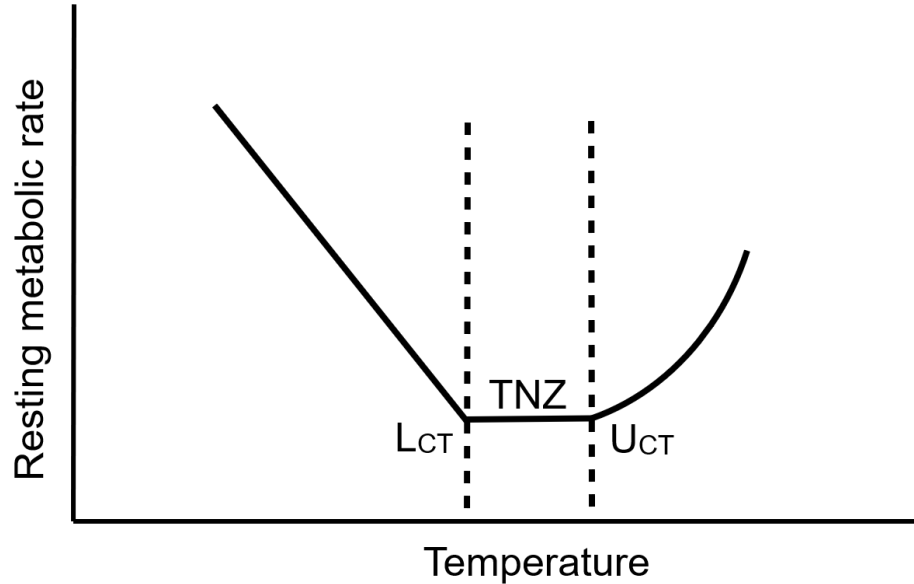


Figure 1: Depiction of a Scholander-Irving Curve. The curve depicts the relationship between temperature and resting metabolic rate of an endotherm. TNZ refers to the thermoneutral zone. LCT and UCT refers to the lower critical temperature and upper critical temperature respectively (Scholander et al., 1950; Levesque, unpublished).

Organisms are fully capable of living in temperatures outside their TNZ, as long as they are able to devote the necessary energy to thermoregulation via an altered energy budget or an increase in resource consumption (Mole et al., 2006; Mitchell et al., 2018). Rising temperatures resulting from global climate change pose the risk of pushing organisms outside, or further outside, their thermoneutral zone, requiring a greater direction of available energy toward thermoregulation (Scholander et al., 1950). If an organism cannot meet the new energy demands, it is forced to move to a cooler environment safely within its TNZ, adapt its thermoregulatory abilities, or perish. All three scenarios carry implications for not only wildlife but also humans, with respect to agriculture, availability of natural resources, and human health.

1.3 Rationale and Objectives

For the reasons previously outlined, it is important to develop mechanistic predictions for how rising temperatures will affect temperate endotherms. North American flying squirrels (genus *Glaucomys*) are wide-ranging, small mammals that occupy a variety of forest types within the temperate zone. Researching the physiological ramifications of high temperatures on flying squirrels can better inform predictive models for these and other species and can improve our understanding of the evolutionary biology of endothermy. Aside from acting as a proxy for larger species, small mammals are also important food resources. Rising temperatures may indirectly affect larger species via diminished prey options even if high temperatures are physiologically tolerable for them.

Flying squirrels, specifically, offer additional advantages as a study species. They are both arboreal and nocturnal – two characteristics not often studied but ones that will experience climate change differently than those of ground-dwelling, diurnal species. This is because nocturnal species rest during the hottest portions of the day and arboreal species often buffer themselves thermally in nests or hollows (Lovegrove et al., 2014). What role these behavioral adaptations will play in their response to rising temperatures is unknown. Additionally, flying squirrels have undergone recent northward range shifts with warmer winter temperatures believed to be the primary driver of these shifts (Bowman et al., 2005; Garroway et al., 2010; Wood et al., 2016). The exact mechanism behind the shifts and its repercussions for forest communities are currently unknown.

I used North American flying squirrels to study thermoregulation of small mammals exposed to high ambient temperatures to better inform mechanistic predictive models. I used metabolic rate and body temperature to investigate two methods of thermoregulation used by

temperate endotherms – increased metabolism and heterothermy. My research objectives were as follows:

Objective 1: Determine the upper limit of thermoneutrality for flying squirrels in Maine and quantify energetics during rest;

Objective 2: Measure free-ranging, core body temperature of flying squirrels during the summer to measure the effects of forest ambient temperature.

CHAPTER 2

STUDY SYSTEM – FLYING SQUIRRELS OF MAINE

2.1 Introduction

2.1.1 Species Description

North America is home to a variety of squirrel species ranging from the common ground and tree squirrels to the more elusive flying squirrels (Steele and Koprowski, 2001). Although rarely seen by humans, flying squirrels (Subfamily Sciurinae, Tribe Pteromyini) occupy the majority of North America. They differ from their ground and tree-dwelling counterparts by possessing the ability to glide from tree to tree and by being nocturnal (Steele and Koprowski, 2001). North America's flying squirrels include: the northern flying squirrel (*Glaucomys sabrinus*), the southern flying squirrel (*Glaucomys volans*), and, the newly discovered, Humboldt's flying squirrel (*Glaucomys oregonensis*, Arbogast et al., 2017). All three are members of the same genus and share the defining characteristics of flying squirrels, but they vary in range, habitat preference, diet, and life history traits.

The northern flying squirrel is the largest of all three species. It occupies much of Canada and several northern states including Minnesota, Michigan, and Maine (Figure 2). It is also found throughout the Pacific Northwest and in isolated patches of the Appalachian Mountains (Figure 2; Wells-Gosling and Heaney, 1984). Northern flying squirrels are primarily found in boreal forests but can occupy mixed coniferous-deciduous forests and, occasionally, broadleaf deciduous forest (Wells-Gosling and Heaney, 1984; Smith, 2007; Weigl, 1977). Lichens and fungi compose a large portion of this species' diet, particularly in the Pacific Northwest where it facilitates the symbiotic relationship between conifers and mycorrhizal fungi (Maser et al., 1978,

Maser et al., 1986). Despite this association, northern flying squirrels can easily diversify to feed on seeds, nuts, berries, insects, and small invertebrates (Wells-Gosling and Heaney, 1984; Smith, 2007).

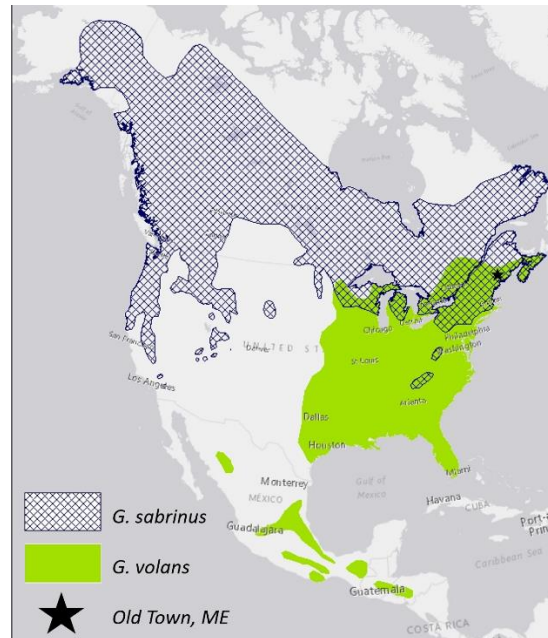


Figure 2: Distribution of *G. sabrinus* and *G. volans* in North America. Maps constructed using spatial data from Cassola, 2016.

Northern flying squirrels do not hibernate, but instead continue foraging throughout the winter. The combination of a thick pelage, well-insulated nests, and the propensity to form aggregations with other conspecifics ensures survival and minimizes thermoregulatory energy expenditure during the winter. There is some evidence of shallow, daily torpor, but its use is minimal compared to other energy-saving thermal strategies (Olson et al., 2016). Mating occurs in late March through May with the first young born in late May through June (Wells-Gosling and Heaney, 1984). One litter, consisting of 2-4 young, is produced per female per year (Wells-Gosling and Heaney, 1984; Smith, 2007). Young are weaned around 2 months of age but remain with the female for some time (Wells-Gosling and Heaney, 1984). Little is known about juvenile dispersal (Smith, 2007). Males typically have larger home ranges than females, <10 hectares

versus <5 hectares, but range size varies with habitat quality and season (Smith, 2007). Primary predators include birds of prey, domestic house cats, foxes, martens and lynx (Wells-Gosling and Heaney, 1984). Northern flying squirrels are a key prey item for the threatened northern spotted owl, *Strix occidentalis caurina*, in the Pacific Northwest, which makes flying squirrels a common target for conservation efforts.

The second species of flying squirrel present in North America is the southern flying squirrel. Southern flying squirrels inhabit much of the eastern half of the United States with isolated populations in Mexico and Central America (Figure 2; Dolan and Carter, 1977). They are present as far northward as New England and southern Quebec, including some areas of sympatry with *G. sabrinus* (Figure 2; Dolan and Carter, 1977; Garroway et al., 2010). Southern flying squirrels primarily occupy temperate to sub-temperate, deciduous forests where hard mast and tree hollows are abundant. They are considered omnivorous and eat a diet consisting of nuts, seeds, berries, insects, small invertebrates and even carrion when necessary (Dolan and Carter, 1977).

Like their northern counterparts, southern flying squirrels do not hibernate over winter but show some evidence of shallow torpor (Olson et al., 2016). They cache food in late fall and make use of tree hollows to provide insulation and to house large aggregations against harsh winter temperatures. Mating takes place in the spring and summer with parturition occurring twice per year – late spring from April to May and early fall from August to September (Dolan and Carter, 1977). Gestation lasts 40 days and the average litter size is 3-4 young (Dolan and Carter, 1977). It is not well known whether a female will give birth during both time periods as young are not weaned until 6-8 weeks and often remain with the mother for longer (Dolan and Carter, 1977). Similarly, juvenile dispersal is not well understood, but *G. volans* are known to be

territorial during mating and rearing season. The average home range in northern New England is 5.7 hectares and 2.6 hectares for males and females respectively (Fridell and Litvaitis, 1991). Predation pressures are similar to those of northern flying squirrels, with owls and domestic cats being the primary threat (Dolan and Carter, 1977).

Lastly, the Humboldt's flying squirrel was discovered in 2017 as a cryptic species of New World flying squirrel. Using mitochondrial DNA, Arbogast et al. (2017) discovered two different clades within the species *G. sabrinus*. The Continental Clade includes northern flying squirrels from North Carolina, Tennessee, West Virginia, Michigan, Idaho, Alberta, Alaska, British Columbia, and Washington, while the Pacific Coastal Clade includes squirrels from British Columbia, Washington, Oregon, and California (Arbogast et al., 2017). Despite their similar geographic range and habitat preference, microsatellite analysis showed no contemporary gene flow between the two clades (Arbogast et al., 2017). Furthermore, comparing both clades to *G. volans* showed that *G. volans* and the Continental Clade are more closely related to each other than either is to the Pacific Coastal Clade (Arbogast et al., 2017). A detailed description of morphology, diet, life history, and behavior does not yet exist for Humboldt's flying squirrel as it has always been classified as *G. sabrinus*.

2.1.2 Shifting Ranges

Aside from their nocturnality and gliding abilities, North American flying squirrels are unique for another reason – their recent, dramatic range shifts northward. Over the past few decades, southern flying squirrels have expanded their range northward in multiple locations as northern flying squirrels contract in the same direction (Bowman, 2005; Wood et al., 2016). Southern flying squirrels have expanded at a rate of 22 km per year between 1994 and 2004 in southern Ontario with concomitant declines in northern flying squirrels (Bowman, 2005). Holt

Forest in southern Maine experienced a complete species turnover from *G. sabrinus* to *G. volans* over an 18-year period (Wood et al., 2016).

No definitive explanation for the observed range shifts has been accepted, but several hypotheses have been proposed, all with climate change at the forefront (Weigl, 1978; Pauli et al., 2004; Bowman, 2005; Smith, 2007; Wood et al., 2015). As average global temperatures rise, both summer and winters months are getting warmer (IPCC, 2014). In the context of flying squirrels, low winter temperatures are thought to define the northern limit of southern flying squirrels (Bowman, 2005; Smith, 2007). With warmer winter temperatures courtesy of climate change, southern flying squirrels may be able to expand into previously uninhabitable areas (Bowman, 2005).

Another proposed hypothesis suggests that changing forest composition permits the northward expansion of southern flying squirrels (Wood et al., 2015). As forests change from the *G. sabrinus*-preferred boreal forests to the *G. volans*-preferred temperate forests, southern flying squirrels may be monopolizing on the expansion of a primary food source – hard mast. However, flying squirrel ranges are shifting much faster than those of arboreal species, and Wood et al. (2015) found little association between forest structure and species' abundance. Additionally, both species have been found outside their associated forest types and even in sympatry with one another (Smith, 2007; Weigl, 1978).

The previous two hypotheses concern the expansion of *G. volans* but do little to address the range contraction of *G. sabrinus*. Two additional hypotheses hinged upon *G. volans*' expansion as the impetus for *G. sabrinus*' contraction have emerged – direct and parasite-mediated competition. In paired nest box experiments, southern flying squirrels have been observed 'driving out' northern flying squirrels and dominating the available tree hollows used

for nest space (Weigl, 1978). Northern flying squirrels are then forced to find nest space in areas without interspecific competition and these areas happen to be northward.

The second hypothesis concerns the nematode parasite, *Strongyloides robustus*. Southern flying squirrels are known to benignly carry *S. robustus* throughout their range, but for northern flying squirrels, the parasite is lethal (Wetzel and Weigl, 1994; Pauli et al., 2004). If warm temperatures allow southern flying squirrels to expand northward and increase their sympatry with northern flying squirrels, *S. robustus* can be more easily transferred between the two species. Additionally, warmer temperatures encourage the persistence of *S. robustus* as it cannot reproduce in temperatures below 5°C (Wetzel and Weigl, 1994). Northern flying squirrels must move to areas unshared by southern flying squirrels or those outside the thermal limits of *S. robustus* if they are to survive.

The aforementioned hypotheses all focus on increased winter temperatures, in one way or another, as the impetus for flying squirrel range shifts. I proposed looking in the other direction, at rising summer temperatures. High temperatures become costly as more energy is directed to cooling and taken away from other vital activities. This energy imbalance can prove fatal in the long run forcing flying squirrels to adapt, move, or perish. I proposed that rising summer temperatures at the southern edge of the northern flying squirrel range have become too energetically costly for northern flying squirrels, and they have moved northward to colder climates to cope. Southern flying squirrels, already accustomed to the heat, move northward to “fill the gap” so to speak. I first needed to locate both flying squirrel species in Maine before testing my hypothesis using flow-through respirometry and free-ranging body temperature.

2.2 Methods

2.2.1 Capture and Processing

Southern flying squirrels were live captured from Dwight B. Demeritt Forest North (44.935° N, 68.682° W) and South (44.940° N, 68.663° W) in Orono/Old Town, Maine from May-November 2017 and May-September 2018. The Dwight B. Demeritt Forest consists of 1,740 acres of mixed forest stands, fields, and water bodies, with the northern and southern portions separated by residential and commercial development. Attempted capture of northern flying squirrels took place at the University of Maine Presque Isle (46.672° N, 68.016° W) and Aroostook Farm (46.654° N, 68.006° W) in Presque Isle, Maine from May-July 2018.

To capture flying squirrels, 30-60 Folding Sherman Sheet Metal Traps (LFA 9 x 3 x 3.5 Folding, Aluminum Trap, Tomahawk Live Trap, Hazelhurst, WI) were placed on the forest floor in a grid pattern. Grids were placed among pine-oak forest patches in both locations and individual traps were placed near large trees if possible. The traps contained cotton balls for nesting material as well as a mixture of peanut butter and rolled oats for bait. Traps were opened around dusk (1800-2000h EDT) and closed within a few hours of sunrise (0500-0800h EDT).

Captured flying squirrels were transferred from the trap into a handling bag to be sexed, weighed, and measured. Morphometric measurements include ear length, hindfoot length (with and without toes), forearm length and reproductive status. Measurements were taken to the nearest millimeter using an electronic caliper and weight to the nearest gram or 0.1 gram using a portable, digital scale (UNIWEIGH Digital Pocket Scale, Cochin, India). All flying squirrels were tagged using ear tags (Mouse Ear Tags, National Band and Tag Company, Newport, KY) and/or passive integrated transponder (PIT) tags (BioThermo13, Biomark, Boise, ID) for

identification upon recapture. Some individuals had a 3 mm biopsy tissue punch taken for genotyping.

All animals used in research (see Chapter 3) were housed at room temperature (~27°C) in the Levesque Lab at the University of Maine for less than 24 hours. When not used in an experiment, squirrels were placed in a ventilated plastic container (Lee's Kritter Keeper, Medium Rectangle, Lee's Aquarium and Pet Products, San Marcos, CA) lined with paper towels and provided apple slices coated with peanut butter. All capture and handling procedures were approved by the University of Maine's Institutional Animal Care and Use Committee Protocol #A2017-03-02 and followed the Wildlife Scientific Collection Permit #2017-516 issued by the State of Maine Department of Inland Fisheries and Wildlife issued to D. Levesque.

2.3 Results

In 2017, 36 southern flying squirrels were captured in Dwight B. Demeritt Forest North and South. No northern flying squirrels were captured in 2017. In 2018, 30 new and 6 previously tagged southern flying squirrels were captured in Dwight B. Demeritt Forest North and South. Only 3 northern flying squirrels were captured at the Presque Isle sites in 2018. Appendix 1 includes measurements taken for captured flying squirrels as well as a categorization of body condition. Body condition is a measure of energy reserves, usually in the form of fat (Schulte-Hostedde et al., 2001). Instead of directly measuring the fat reserves of captured individuals, the ratio between body mass and forearm length was used as an index of condition (Schulte-Hostedde et al., 2001). Individuals with a positive index have greater energy reserves and are in good condition compared to those with a negative index that have few fat reserves.

2.4 Discussion

Contrary to expectations, only southern flying squirrels were captured in Dwight B. Demeritt Forest North and South in 2017. Personal communications and species distribution maps led us to believe that Orono/Old Town, Maine would primarily house northern flying squirrels (Figure 2). Although species turnover has occurred in Maine, it was seen much farther south at Holt Forest Research Station (43.869° N, 69.776° W) located in Arrowsic, Maine (Wood et al., 2015). The documented turnover from northern flying squirrels to southern flying squirrels occurred between 1986-2004 (Wood et al., 2015). Orono/Old Town, Maine is a full degree of latitude north of Holt Forest, indicating the southern species further expanded northward at a rate of ~8.5 km/yr. Similar rapid movements have been documented elsewhere in North America (Bowman et al., 2005; Garroway et al., 2010). As previously mentioned, southern Ontario witnessed a northward range expansion of 22 km/yr from 1994-2004 for southern flying squirrels (Bowman, 2005).

The presence of southern flying squirrels in Dwight B. Demeritt Forest North and South does not negate the possibility of northern flying squirrels living in other forests at a similar latitude. The Demeritt Forests are both managed by the University of Maine and have been for more than 50 years. The mixed forests, used for forestry demonstration, education, research, and community recreation, can provide suitable habitat for either species of flying squirrel. Nearby is the Penobscot Experimental Forest (44.851° N, 68.628° W) in Bradley/Eddington, Maine where northern flying squirrels are still captured, though rather infrequently (A. Brehm and A. Mortelliti, personal communication). The Penobscot Forest lies in a transitional zone between eastern broadleaf and boreal forests and contains mostly mixed-species, northern conifers. The Penobscot Forest more closely resembles the forest type associated with northern flying

squirrels, which could explain their persistence here. As climate change progresses, the Penobscot Experimental Forest may transition to a mixed, hardwood forest like Dwight B. Demeritt Forest North and South, ridding central Maine of its northern flying squirrel populations completely.

Species turnover has been one consequence of flying squirrel range shifts, and hybridization has been another. Garroway et al. (2010) suggest that as southern and northern flying squirrels become more sympatric due to climate-driven range shifts, incidence of hybridization between these two species will increase. Low densities of southern flying squirrels at the leading edge of their range expansion can lead to reduced mating options and/or insufficient aggregations for winter thermal regulation (Garroway et al., 2010). If southern flying squirrels are to maintain fringe populations, they may need to rely on northern flying squirrels for mating or social thermoregulation which will increase the incidence of hybridization (Garroway et al., 2010). A similar scenario is possible in Maine. The individuals captured for this research were identified phenotypically as southern flying squirrels, but they could carry genetic markers of the northern species. The next step in this research is to verify species identification genetically to see if any hybridization has occurred in either Demeritt Forest location. Karyotyping is currently underway, and results are expected by summer 2019.

My primary hypothesis about the role that high summer temperatures play in guiding flying squirrel range shifts pertains primarily to the northern species, which we were not able to capture in sufficient numbers. However, the northward expanding southern species still provides new fodder for thermal physiology research. Fringe populations can differ from core populations morphologically, ecologically, and even genetically given enough separation and isolation. The summer heat might not be limiting southern flying squirrels in Maine, but this population will

certainly react differently to heat than populations residing in the southern United States or Mexico. Understanding the thermal strategies of southern flying squirrels at the northern edge of their expansion offers a unique comparison to previous research and can provide insight into what other expanding populations are or will be experiencing as temperatures continue to rise.

CHAPTER 3

THERMOPHYSIOLOGY OF SOUTHERN FLYING SQUIRRELS

3.1 Introduction

With southern flying squirrels found as far south as Mexico and as far north as Maine, it is no surprise that individual- and population-level differences exist in estimations of thermoregulatory capacity (Stapp, 1992). However, all previous studies have focused on thermoregulation at cold temperatures with little attention paid to the effects of high temperatures (Pearson, 1947; Neumann, 1967; Muul, 1968; Stapp, 1992; Olson et al., 2017). Just as southern and northern populations of *G. volans* react differently to cold temperatures, they may react differently to high temperatures as well (Stapp, 1992). Populations of *G. volans* at the northern edge of their range expansion seldom experience the hot, arid conditions to which southern populations are accustomed and are, therefore, not immune to the heat. IPCC models predict Maine's average temperature will increase 1.1-1.7°C between now and 2050 and that the number of excessively hot and humid days (heat index > 35°C) will triple in portions of the state over the same time period (Fernandez et al., 2015). To explore the effects of Maine's rising temperatures on the thermoregulatory physiology of southern flying squirrels, I measured energy usage and body temperature of southern flying squirrels exposed to high ambient temperatures.

I focused on two thermoregulatory strategies used under high heat conditions: elevation of metabolic rate (increased energy usage) and use of heterothermy (variation in core body temperature with ambient conditions). To determine metabolic rate across a range of temperatures, I used flow-through respirometry to measure oxygen consumption and carbon dioxide production (Withers, 2001; Lighton, 2008). Additionally, I measured evaporative water

loss and subcutaneous body temperature as other indicators of thermoregulation. I predicted that metabolic rate and evaporative water loss would increase with ambient temperature after surpassing the UCT (some ambient temperature $\leq 40^{\circ}\text{C}$). To detect the use of heterothermy, I measured core body temperature of southern flying squirrels during the warm summer months. I hypothesized that daytime forest temperatures would, in part, determine the body temperature of *G. volans* during its inactive phase.

3.2 Methods

3.2.1 Respirometry

3.2.1.1 Animal Handling

All flying squirrels were captured and measured as outlined in Chapter 2. Flying squirrels used for resting metabolic rate experiments were all adult males or non-reproductive adult females. All squirrels were brought back to the Levesque Lab and housed for 1-5 hours until placed in the respirometry chamber. In 2017, all squirrels were fasted before entering the respirometry chamber to satisfy the requirement that post-absorptive animals be used to measure basal metabolic rate (Withers, 1992). However, fasted squirrels were less apt to rest in the metabolic chamber, and many experiments were cut short due to high locomotor activity or the persistence of stress behaviors. In 2018, squirrels were fed a small slice of apple upon their arrival to the lab. Fed squirrels settled down more quickly inside the chamber and exhibited fewer stress behaviors throughout the experiment. I was primarily interested in resting metabolic rate rather than basal metabolic rate because of its applicability to wild conditions (Withers, 1992). Additionally, the respirometry quotient between fasted and fed animals were roughly equivalent, indicating that the two methods were comparable.

All squirrels were weighed to the nearest gram or tenth of a gram before and after each experiment. Squirrels were removed from the chamber if they showed signs of distress, reached a subcutaneous temperature of 41°C, or remained too active for more than 120 minutes. All squirrels were fed with apple and peanut butter after the completion of respirometry experiments and returned to their location of capture.

3.2.1.2 Flow-Through Respirometry Set-Up

The metabolic chamber was a 1.9L airtight, plastic container (Lock and Lock Co., Seoul, South Korea) with 3 ports: one for the incurrent airstream, one for the excurrent airstream, and one for a temperature sensor (Compression Push Fitting, BrassCraft, Masco, Michigan). A mesh wire grate kept the squirrel elevated above the temperature sensor and inflow ports. Mineral oil (99.99% or higher) was placed in the bottom of the container, below the grate, to absorb any urine or feces produced by the animal (Figure 3).



Figure 3: *Glaucomys volans* in metabolic chamber used for respirometry experiments.

Temperature inside the metabolic chamber was monitored using a thermocouple and meter (TC-2000 Type-T Thermocouple Meter, Sable Systems, North Las Vegas, NV) and recorded with two temperature data loggers (DS1922L Thermochron iButtons, Maxim Integrated, San Jose, CA) attached to the chamber base and lid. Subcutaneous temperature of the squirrel was monitored via pit-tag (Chapter 2) and recorded using a Biomark HPR Plus Reader (Biomark Inc., Boise, ID). Additionally, an infrared USB camera recorded the squirrel's activity and allowed for non-disruptive monitoring during the experiment.

With the squirrel inside, the metabolic chamber was placed in either a temperature-controlled cabinet (Incubator, Refrigerated with Mechanical Convection, KB 53, BINDER, Long Island, New York) or cooler (Pelt-5, Sable Systems, North Las Vegas, NV) depending upon equipment availability. The incurrent air used for flow-through respirometry was pulled from outside the building whenever possible. If the lab set-up prohibited the use of outside air, air was drawn directly from an air vent. The incurrent airstream was pulled through a column containing the desiccant Drierite ($\geq 98\%$ CaSO₄, $< 2\%$ CoCl₂, W. A. Hammond Drierite Co. Ltd., Xenia, OH) by a 1.0 L/min pump. Once dried, the incurrent air was divided into two airstreams – one for the chamber and one for the control stream. Gas mass flow controllers (MC-Gas Mass Flow Controllers, Alicat Scientific, Tucson, AZ) regulated the incurrent airflow to within 0.8% of the desired flow rate. The chamber flow rate ranged between 500-1650 ml/min., depending on chamber humidity, and the control flow rate ranged between 1000-2500 ml/min.

After the gas mass flow controller, the incurrent air entered the cooler box or cabinet housing the metabolic chamber. The incurrent air passed through a coil of copper tubing to equilibrate its temperature to that of the cooler box/cabinet before entering the metabolic chamber via the incurrent port. Air passed through the chamber and exited through the excurrent

port before entering a gas flow switcher (BL-2 Baseline System or RM-8 Flow Multiplexer, Sable Systems, North Las Vegas, NV). The gas flow switcher automatically alternates which airstream, control or chamber, is passed downstream to the gas analyzers. It sampled the control stream for 5 minutes and the chamber stream for 40 minutes. The sampled air stream is pulled through the gas analyzers, carbon dioxide then oxygen, via a second pump (SS-4 Sub-sampler, Sable Systems, North Las Vegas, NV) before finally exiting the system. A water and carbon dioxide gas analyzer was used for every experiment (LI-840A CO₂/H₂O Gas Analyzer, LI-COR, Lincoln, NE) and an oxygen analyzer (FC-10 Oxygen Analyzer, Sable Systems, North Las Vegas, NV) was used whenever possible. The excurrent airstream was scrubbed of water and, on a few occasions, carbon dioxide after passing through the CO₂/H₂O analyzer but before the oxygen analyzer to ensure the accurate measurement of oxygen values. The LI-840A was calibrated every six months at a minimum; it was zeroed using medical grade oxygen (Matheson Tri-Gas, Basking Ridge, NJ) and spanned using 1.95% CO₂ certified span gas (Matheson Tri-Gas, Basking Ridge, NJ).

3.2.1.3 Experimental Protocol

Respirometry measurements were conducted at chamber temperatures ranging from 20-40°C. Flying squirrels were exposed to a maximum of four temperatures during a trial. Some flying squirrels were used for multiple trials, but all trials were conducted after different capture events. If a squirrel was used for multiple trials, it was exposed to different temperatures each time. The first temperature upon entering the metabolic chamber was 20, 25, or 30°C and the squirrel remained at this temperature for a minimum of 2 hours. Once a squirrel was consistently resting, chamber temperature was increased by no more than 10° increments between 20-30°C and 4° increments between 30-40°C. Squirrels were kept at each new temperature for a minimum

of 1 hour. Chamber temperature was always increased, never decreased, over the course of an experiment. An example temperature ramping is shown in Figure 4. Following the protocol developed by the ‘Hot Birds Project’ (McKechnie et al., 2016; Whitfield et al., 2015), humidity within the chamber was kept below 15 ppt by adjusting the flow rate as needed (500-1650 ml/min). Experiments ranged from 4-8 hours depending on the behavior of the squirrel and the number of temperatures tested.

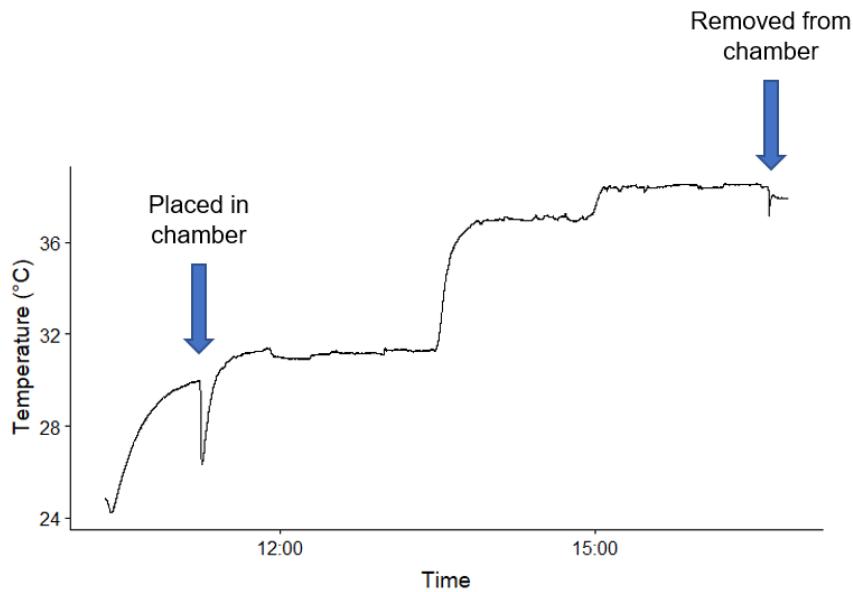


Figure 4: Chamber temperature over the course of an experiment. Squirrel was placed in the chamber at ~1100 and removed at ~1700. Experimental temperatures were 30, 36, and 38°C.

3.2.1.4 Data Analysis

Oxygen, carbon dioxide, water vapor, and analyzer cell pressure measurements were recorded every second using ExpeData-P Analysis Software (Sable Systems, North Las Vegas, NV) and LI-840A Software (LI-COR, Lincoln, NE). For each 40-minute stretch of chamber measurements, the lowest, continuous 5-minute period of carbon dioxide production was isolated using Expedata. A custom macro first selected the lowest 1200 carbon dioxide values and, from that, the 600 most stable values (equal to 5 minutes) before calculating the mean and standard

deviation of carbon dioxide, water vapor, and cell pressure. Measurements of oxygen (if applicable), flow rate, chamber temperature, and subcutaneous temperature were matched to each 5-minute period.

All measurements of oxygen consumption and carbon dioxide production were transformed into $\dot{V}O_2$ and $\dot{V}CO_2$ using Equations 1 and 2 (See below; Withers, 2001). The respiratory quotient (RQ), $\dot{V}CO_2/\dot{V}O_2$, was calculated for every selected 5-minute period in a single trial (Withers, 2001). RQ values were then averaged across all periods and all trials to generate a single RQ value for flying squirrels. The generated RQ of 0.7 was used to solve for $\dot{V}O_2$ and $\dot{V}CO_2$ for experiments lacking the oxygen analyzer (See below Equations 3 and 4; Withers, 2001). Resting metabolic rate (RMR) was calculated using Equations 5 and 6 (See below; Lighton, 2008). Water vapor concentration was transformed into water vapor density (WVD), evaporative water loss (EWL), and, ultimately, evaporative heat loss (EHL) using Equations 7-10 (See below; Withers, 2001; Withers, 1992).

(1)

$$\dot{V}O_2 = Flow\ Rate * \frac{((F_iO_2 - F_eO_2) - F_eO_2 * (F_eCO_2 - F_iCO_2))}{(1 - F_eO_2)}$$

$\dot{V}O_2$ = volume of oxygen consumed, F_eO_2 = excurrent concentration of oxygen, F_iO_2 = incurrent concentration of oxygen, F_eCO_2 = excurrent concentration of carbon dioxide, F_iCO_2 = incurrent concentration of carbon dioxide

(2)

$$\dot{V}CO_2 = \frac{Flow\ Rate * (F_eCO_2 - F_iCO_2) - (F_eCO_2 * \dot{V}O_2)}{(1 - F_eCO_2)}$$

$\dot{V}O_2$ = volume of oxygen consumed

(3)

$$\dot{V}CO_2 = \frac{\text{Flow Rate} * (F_e CO_2 - F_i CO_2)}{1 - F_e CO_2 * (1 - (\frac{1}{RQ}))}$$

(4)

$$\dot{V}O_2 = \frac{\dot{V}CO_2}{RQ}$$

(5)

$$\text{Energetic Equivalence of } O_2 = 16 + 5.164 * RQ$$

(6)

$$RMR = \frac{\dot{V}O_2 * \text{Energetic Equivalent}}{60}$$

(7)

$$VP = \frac{H_2O * BP}{8.3143 * (T_a + 273)}$$

H_2O = excurrent water concentration, BP = barometric pressure, T_a = ambient temperature.

(8)

$$WVD = \frac{VP * 18.01528}{1000}$$

(9)

$$EWL = WVD * \text{Flow Rate}$$

(10)

$$EHL = EWL * 2.43 \text{ JmL}^{-1}O_2$$

Some trials yielded multiple 5-minute periods of low metabolic rate for a given temperature because squirrel activity and/or chamber warming time necessitated longer exposure to a given temperature. To select the best estimate of resting metabolic rate at a given temperature, each 5-minute period was subjected to exclusion tests. Exclusion tests included the following: all measurements taken within the first hour of the experiment, while the squirrel adjusted to the chamber, were excluded. Any measurements taken within an hour of a major disruption (i.e. equipment failures or adjustment, building construction, fire alarms) were excluded for similar reasons. Additionally, periods in which the squirrel exhibited increased

activity were excluded. Increased activity was detected in one of two ways: through visual confirmation using video recordings of the experiment or through comparison of metabolic rate standard deviations. Each experiment was broken up into 10-minute increments for which standard deviation of carbon dioxide was determined. Standard deviations were averaged across each 40-minute chamber recording and compared to those of known activity periods as identified by video records. Averaged standard deviations that were equal to or above those of active periods were excluded. If multiple 5-minute periods remained after all exclusion tests, the values were averaged to generate one resting metabolic rate measurement for each experimental temperature to be used for subsequent analyses.

To generate an estimate of the upper critical temperature (UCT) for southern flying squirrel, resting metabolic rates and ambient temperatures for all experiments were plotted using R Packages 'ggplot2' and 'cowplot' (Wickham, 2016; Wilke, 2018). The piecewise linear regression analysis using the R Package 'segmented' was applied to the best fitting model to determine its breakpoints, indicating the lower or upper critical temperature, within a 95% confidence interval (Muggeo, 2008). Linear models were developed using the R Package 'nlme' to evaluate the effects of various factors on metabolic rate and compared using Akaike Information Criterion (AIC_c) scores and Akaike weights (AIC_cWt) generated from the 'AICcmodavg' package (Appendix 2; Mazerolle, 2017; Pinheiro et al., 2018). Evaporative water loss, subcutaneous temperature, and the ratio of evaporative heat loss to metabolic heat production were all evaluated against ambient temperature. They were then subjected to model testing and subsequent breakpoint determination.

3.2.2 Core Body Temperature

3.2.2.1 Animal Handling

Only male southern flying squirrels were used in the body temperature experiments to avoid negatively impacting reproductive females. Additionally, squirrels had to weigh ≥ 60 g to ensure that the logger and radio collar did not weigh $>10\%$ of total body weight. Flying squirrels that met these requirements were brought to the Levesque Lab and held in a plastic container prior to surgery. Following IACUC approved methods, they were given ~ 0.01 g of Capofran analgesic delivered on a slice of apple 2 hours before and immediately after surgery to minimize pain. All squirrels were weighed to the nearest gram before and after each surgery.

3.2.2.2 Surgical Implantation

Implantation surgeries took place between 0800 and 1600h EDT in July of 2017 and May-June of 2018. The temperature sensitive data loggers used to collect core body temperature data were of two varieties: a 1 g hermetically sealed, ceramic data logger (DST nano-T, STAR:ODDI, Gardabaer, Iceland) and a 3-4 g custom made data logger (Gerhard Fluch, University of Veterinary Medicine, Vienna, Austria) coated in epoxy and a layer of surgical wax (Paramat Extra-Merck KGaA, Darmstadt, Germany). Both recorded date, time, and core body temperature every five minutes for the duration of deployment. The STAR:ODDI loggers were hermetically sealed and biocompatible while the Fluch loggers required encapsulation in surgical wax to be biologically inert. All loggers were sterilized in Isopropyl alcohol for a minimum of 4 hours prior to implantation.

Squirrels were placed in an air-tight, plastic container for sedation via vaporized Isoflurane (Isoflurane, USP, Piramal Healthcare, Inc., Bethlehem, PA). A 5% concentration of Isoflurane was administered at a rate of 700-800 ml/min until the squirrel could no longer right

itself and appeared to be sedated. The squirrel was then removed from the chamber and a small mask applied to its face to continue administering Isoflurane at a 2-3% concentration for the duration of the surgery.

The ventral surface was prepped for incision by shaving a 3 cm x 5 cm section of fur and cleaned with a betadine scrub, isopropyl alcohol, and a betadine solution (Betadine Surgical Scrub (povidone-iodine, 7.5%) and Betadine Solution (povidone-iodine, 10%), Purdue Pharma L.P., Stamford, CT). Once cleaned, a small incision was made, not exceeding 2 cm, in the skin and abdominal muscle tissue along the linea alba. The temperature sensitive data logger was placed inside the intraperitoneal cavity and the incision was sealed with dissolvable sutures (Coated VICRYL (Polyglactin 910) Suture, Ethicon, Inc., Bridgewater, NJ) and tissue glue (Vetbond Tissue Adhesive, 3M, St. Paul, MN). An antibacterial ointment (Neosporin Antibacterial Ointment, Johnson & Johnson Consumer Inc., New Brunswick, NJ) was applied to the surgical site to prevent infection.

After completing the surgery, but while the squirrel was still sedated, radio collars were attached. Radio transmitters (~4g, PD-2C Trasmitters, Holohil Systems Ltd., Ontario, Canada) were coated in epoxy for durability and collar wires were tucked inside rubber tubing to prevent skin irritation. Radio collars were fit large enough to rotate around the neck but not large enough to place a limb through. If the squirrel was not previously tagged (See Chapter 2), an ear tag and PIT tag in the interscapular region were added. A biopsy punch was taken from the left ear of each squirrel that underwent surgery and additional morphometric data (snout-vent length, urogenital distance, tail length, and total body length) was collected.

Flying squirrels were moved to a clean container beneath a heat lamp for recovery. Additional food and analgesic were provided as they recovered from surgery. Individuals were

kept in the lab overnight for observation and released at the capture site the next morning. Attempts were made to recapture implanted individuals throughout the field season to monitor recovery and collect respirometry data. The same procedure outlined above was used to recover the data loggers. Implanted flying squirrels were euthanized via an Isoflurane overdose and cervical dislocation after logger recovery surgery.

3.2.2.3 Forest Temperature

To provide context for the body temperature data and to determine its effect on body temperature, ambient temperature data were collected every 45 minutes in the Dwight B. Demeritt Forest North and South from June-November 2017 and May-September 2018. Temperature-sensitive data loggers (DS1922L Thermochron iButtons, Maxim Integrated, San Jose, CA) contained inside 500 ml matte black plastic bottles were placed at three heights in each forest – tied to a tree 3 meters above the ground, affixed to the base of the tree, and buried 10-15 cm below the soil surface at the base of the tree. Additionally, one Tinytag logger (Tinytag Plus 2 TGP-4500, Gemini Data Loggers, Chichester, West Sussex, United Kingdom) placed at ground level near the base of a tree recorded temperature and relative humidity in Dwight B. Demeritt Forest North.

3.2.2.4 Data Analysis

Body temperature (T_b) was recorded every 5 minutes for the duration of deployment. Before analysis, all data from the first week of deployment and anytime the animal was brought to the lab for respirometry experiments were removed. Each body temperature record was matched to an ambient temperature (T_a) record and categorized as daytime or nighttime according to sunrise and sunset times in the eastern time zone using the ‘maptools’ package in R (Bivand and Lewin-Koh, 2018). Additionally, a squirrel-defined date running from dusk to dusk

was assigned to each record. The squirrel-defined date remedied the issue of splitting a nocturnal animal’s activity period into two separate calendar days and allowed me to examine the entire activity period as one unit.

Combing the daytime/nighttime categorization and the squirrel-defined date, the ‘ddply’ function within the R Package ‘plyr’ extracted the mode T_b and T_a , the average minimum and maximum T_b and T_a , and the min-max T_b and T_a range for each resting and active period throughout the time series (Wickham, 2011). To determine the factors influencing body temperature, particularly the summary statistics extracted through ‘plyr’, linear models were developed and compared using AIC_c scores and AIC_cWt (Appendix 3).

Lastly, an additional measure of T_b variation, the Heterothermy Index (HI), was applied to each squirrel’s body temperature. The HI metric calculates the magnitude of a heterothermic response in relation to the active T_b mode during a given time frame, much like a modified standard deviation (Boyles et al., 2017). HI values can be compared between individuals, populations, or species over any time period to quantify the degree of heterothermy exhibited.

3.3 Results

3.3.1 Resting Metabolic Rate

In total, 10 individuals were used for respirometry experiments in 2017 and 12 were used in 2018. From those 22 squirrels, 53 resting metabolic rate (RMR) data points spanning 20-40°C were used to estimate the upper critical temperature (UCT) of southern flying squirrels (Table 1).

Table 1: Southern flying squirrels used for respirometry experiments. The date, sex, start weight, and experimental temperatures are shown. *Indicates squirrel was used for multiple trials.

Squirrel ID	Date	Sex	Weight (g)	Temperatures (°C)
UM003	5/21/2017	M	79.2	30

Table 1 Cont.

UM007	5/29/2017	M	64.8	25, 30
UM008	5/29/2017	M	59.6	34
UM012	7/24/2017	M	53	30, 32
UM015	7/27/2017	M	59	34, 38
UM796*	7/31/2017	M	53	30, 36
UM020	8/1/2017	F	55	25, 34, 36, 38
UM028	8/2/2017	F	51	30
UM031	11/15/2017	M	70.2	30, 34
UM052	6/11/2018	F	53.6	25, 32
UM073*	6/12/2018	M	61	30, 32, 36
UM071	6/21/2018	F	49.1	25, 30
UM780*	8/2/2018	F	54	30, 38
UM073*	8/6/2018	M	75.3	25, 36, 38, 40
UM740	8/7/2018	M	65	30, 32, 38
UM075	8/11/2018	F	65	25, 32
UM076	8/12/2018	M	71	32, 34
UM796*	8/24/2018	M	57.2	20
UM783	8/26/2018	F	60.4	20, 25, 30
UM718	8/29/2018	F	61.6	20, 25, 30
UM780*	8/30/2018	F	51.7	20, 30, 32
UM802	9/1/2018	M	66.7	36, 38, 40
UM772	9/8/2018	F	56.3	30, 36, 38

The best fitting model for estimating resting metabolic rate included ambient temperature and mass as predictor variables (Appendix 2). This model was subsequently used in breakpoint estimation. The 'breakpoint' function in the 'segmented' package only detected the LCT at 29.8°C (95% CI: 27.49-32.10°C – Figure 4a) and no break point at a higher temperature which would have indicated the UCT.

Using the same best fitting model (See Appendix 2), breakpoints were determined for evaporative water loss (EWL), subcutaneous temperature (T_{sub}), and the ratio of evaporative heat loss to metabolic heat production (EHL/MHP). The breakpoints and their 95% confidence intervals are as follows: EWL = 36.22°C (35.16-37.28°C), T_{sub} = 33.64°C (31.54-35.73°C), EHL/MHP = 36.58°C (35.46-37.7°C) (Figure 4b-d).

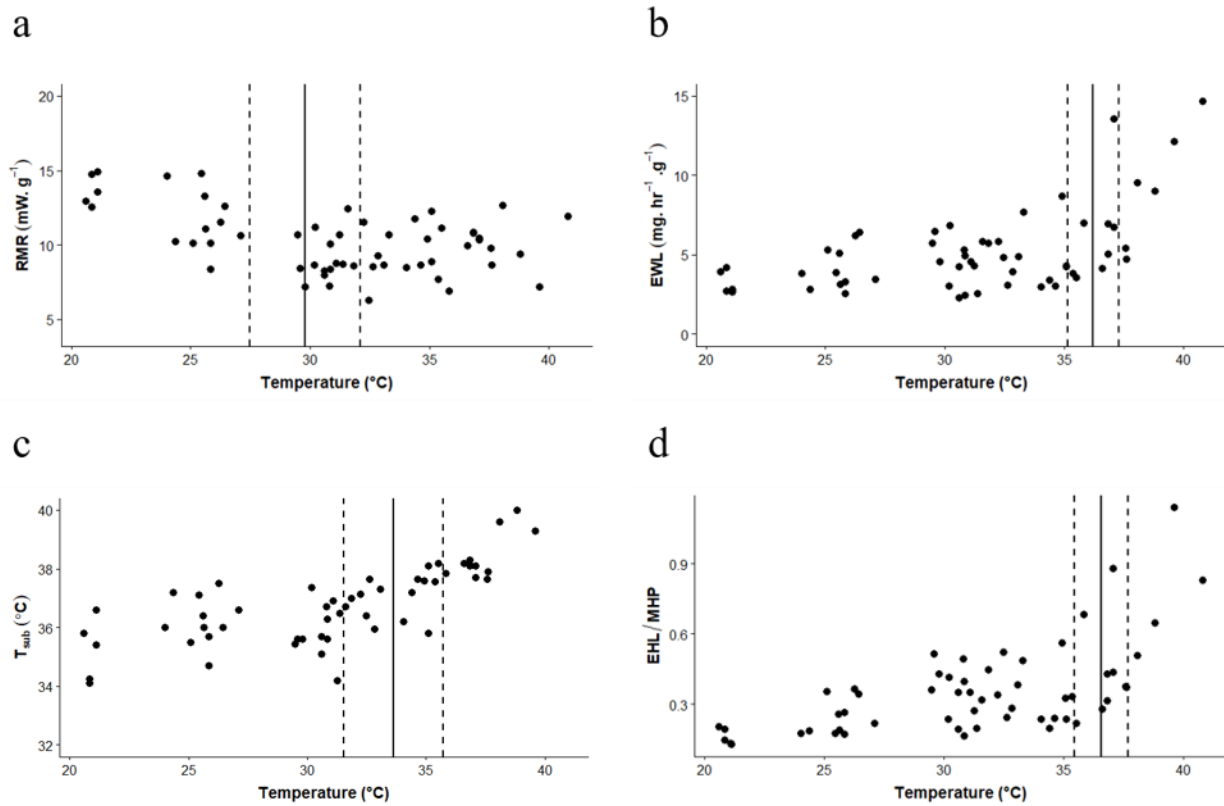


Figure 5: Physiological parameters of *G. volans* exposed to various ambient temperatures. Breakpoint estimate drawn as solid black lines and 95% confidence intervals as dashed lines. a) Resting metabolic rate in milliwatts per gram, b) Evaporative water loss in milligrams per hour per gram, c) Subcutaneous temperature in °C, d) Ratio of evaporative heat loss to metabolic heat production.

3.3.2 Core Body Temperature

Two flying squirrels were implanted with data loggers in 2017 and five in 2018 with one data logger recovered in 2017 and four in 2018 (Table 2). One of the loggers recovered in 2018 was found in a recently deceased individual. Data from the month preceding the recovery were omitted to reduce the influence of any condition that may have contributed to death.

Table 2: Southern flying squirrels used for core body temperature experiments. The start weight, date of temperature-sensitive data logger implantation and retrieval are shown. *Recovered from deceased individual.

Squirrel ID	Mass (g)	Implantation Date	Retrieval Date	Total Days Deployed
UM031	62	4 Aug. 2017	15 Nov. 2017	103
UM073	65	8 May 2018	6 Aug. 2018	90
UM076	63	9 June 2018	12 Aug. 2018	64
UM726	61	8 May 2018	13 Aug. 2018*	97
UM802	63	22 June 2018	1 Sept. 2018	71

Body and ambient temperature traces varied over the course of deployment (Figure 6).

Flying squirrels show a clear pattern of T_b fluctuation matching their daily activity cycle: high T_b during the active nighttime phase and a lower T_b during the resting daytime phase (Figures 6-7). The modal T_b for active squirrels is 39.94°C and for resting squirrels is 37.5°C (Figure 8). Daily variation in body temperature was quantified using the Heterothermy Index which revealed an all-squirrel, daily, average HI value of 1.93 (Table 3).

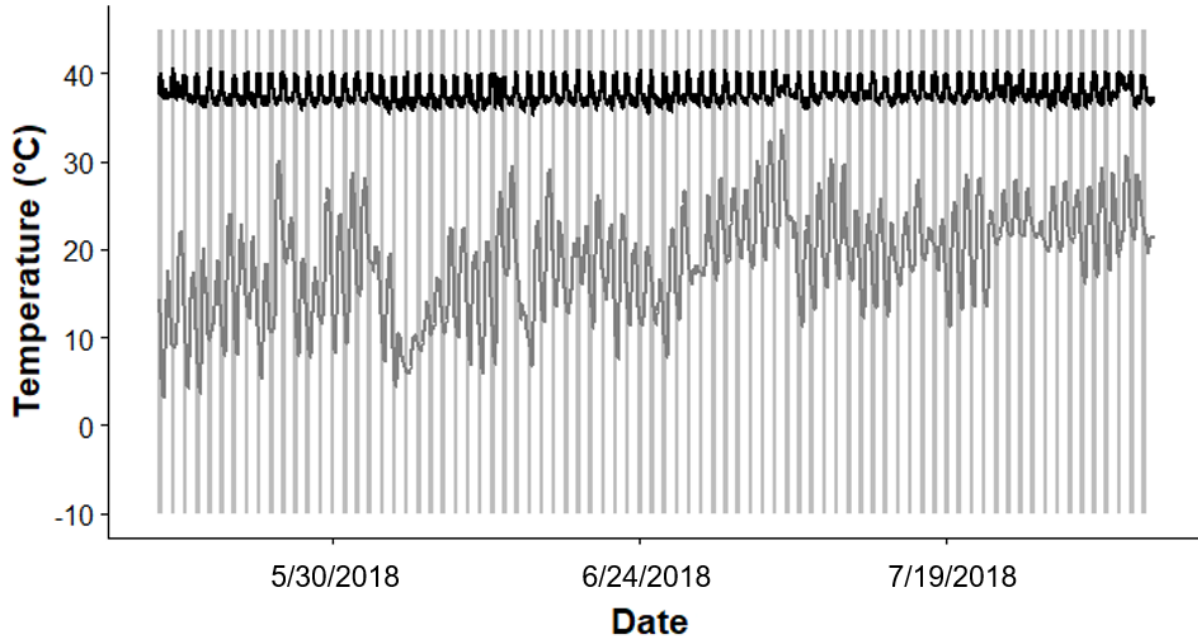


Figure 6: Core body and ambient temperature traces. Flying squirrels exhibit a stable circadian rhythm of body temperature despite fluctuating ambient temperature. Black line shows core body temperature of UM073 and grey line shows ambient temperature of Dwight B. Demeritt Forest South. Temperatures collected from 15 May 2018 to 4 August 2018. White bars indicate daylight hours and grey bars nighttime hours.

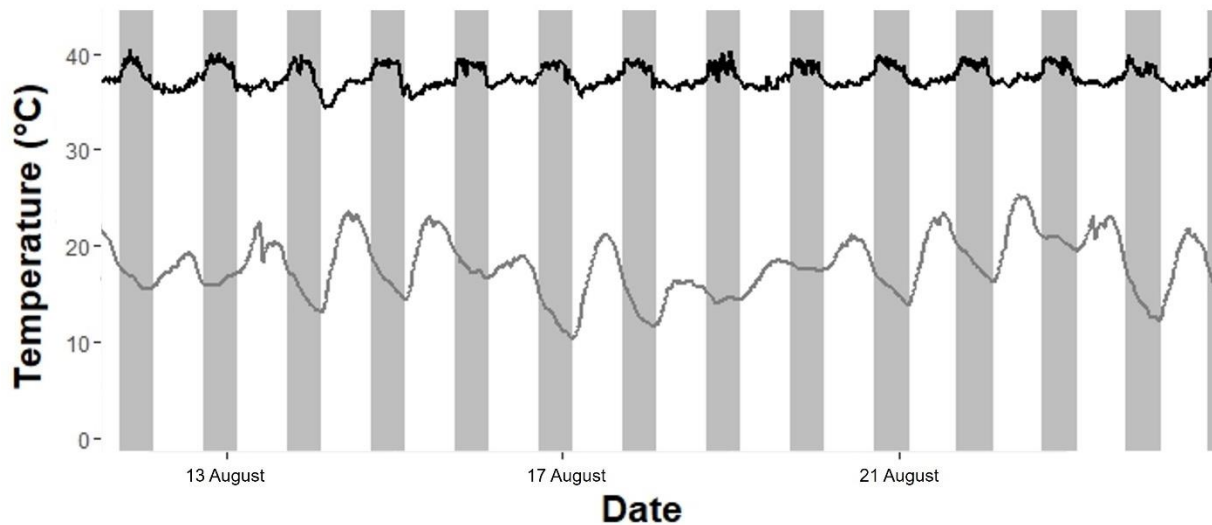


Figure 7: Excerpt of core body temperature trace. Black line shows core body temperature of UM031 and grey line shows ambient temperature of Dwight B. Demeritt Forest North. Temperatures collected from 12 August 2017 to 25 August 2017. White bars indicate daylight hours and grey bars nighttime hours.

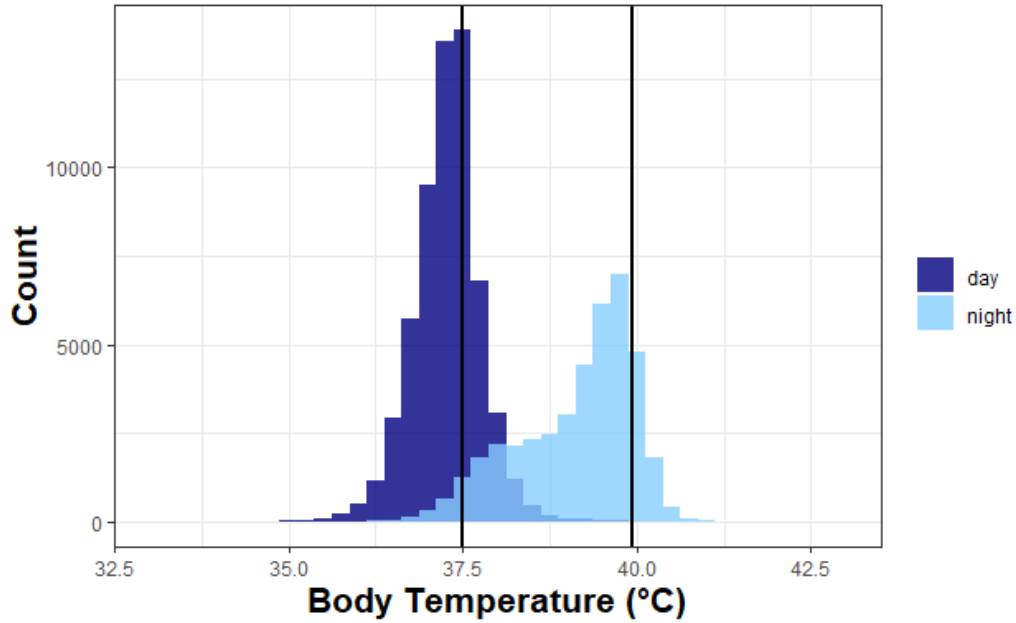


Figure 8: Histogram of core body temperature for all implanted *G. volans*. Vertical black bars represent active (nighttime) and resting (daytime) modal T_b .

Table 3: Heterothermy Index for *G. volans* individuals.

Squirrel ID	HI Value
UM031	1.92
UM073	1.94
UM076	2.20
UM726	1.79
UM802	1.86

Model testing revealed the significant driver of average maximum body temperature to be day of the year, with average maximum ambient temperature included in comparably strong models (Appendix 3). Both day of the year and average minimum ambient temperature were significant predictor variables of average minimum T_b in the best fitting model (Appendix 3).

Like average maximum T_b , the average T_b range was best predicted by day of the year, with ambient temperature range being a significant variable in comparable models (Appendix 3).

3.4 Discussion

The estimated lower critical temperature (LCT) of 29.8°C falls within the range of estimations from previous studies (27.6-35°C; Stapp, 1992). However, two issues must be considered before comparing my LCT estimate to others. First, I used a wide sampling interval across cooler temperatures which led to a large 95% confidence interval for my estimate (27.49-32.10°C). Previous studies sampled at intervals <5°C (Stapp, 1992). Second, I chose to use resting metabolic rate (RMR) instead of basal metabolic rate (BMR) in my experiment. RMR does not require the animal to be fasted prior to metabolic measurements, and I found that fed squirrels were less active than fasted squirrels while inside the metabolic chamber. Although similar, RMR can be substantially higher than BMR, and may even double it in value under certain conditions (Withers, 1992). I chose to use RMR because it is more comparable to conditions experienced by a wild flying squirrel and would ultimately result in a more realistic predictive model (Larivée et al., 2010; Withers et al., 2016).

At the warmer end of my sampling range, I did not detect a breakpoint (upper critical temperature) in metabolic rate in animals exposed to temperatures as high as 40°C. There are two explanations for this result – either I did not test the squirrels at high enough temperatures or there is no UCT for metabolic rate. The first explanation is unlikely as individuals exposed to this temperature showed visible signs of heat stress and a higher-than-average subcutaneous temperature. The second explanation is plausible depending on my definition of UCT. The traditional definition of UCT is the temperature at which metabolic rate rises above basal level, but, more recently, UCT has been defined as the temperature at which evaporative cooling starts

(Withers, 1992; Withers et al., 2016; Mitchell et al., 2018). I detected no UCT when looking at RMR but did identify an UCT based on evaporative water loss (EWL) at 36.2°C. The EWL-defined UCT was also accompanied by the postural changes and increased body temperature.

The disparity between these estimates of UCT – nonexistent versus 36.2°C – begs the question, is the UCT ecologically relevant? Measuring metabolic rate in the laboratory using flow-through respirometry has been criticized for its limited relevance to natural conditions (Mitchell, 2018). BMR, the most commonly used metric, requires an animal to be mature, fasted, non-reproductive, and resting – conditions that rarely co-occur in the wild (Withers, 1992; Withers et al., 2016). If individuals rarely meet all of these requirements, it is difficult to determine how accurate estimations of UCT actually are. Similarity to wild conditions aside, there is evidence that UCT, no matter how it is defined, is not a thermal limit of any consequence (White and Seymour, 2004; Mitchell et al., 2018). As Mitchell et al. (2018) point out, animals constantly experience ambient temperatures above their UCT and continue to thrive individually and as a species. As long as an animal has enough resources (water, food, time, a place to escape from the heat – even momentarily) to compensate for the above-basal-level metabolic rate, it can continue to live under higher temperatures indefinitely.

Furthermore, the state of Maine is far less likely to see temperatures above 36°C than other parts of the world. Although the number of extremely hot and humid days is expected to increase, even the southernmost portions of the state will only see ~15 of these days by the 2050s (Fernandez et al., 2015). Unless coincident with widespread disease or a severe drop in resources, the majority of flying squirrel individuals can most likely compensate for the higher energy usage needed to cool themselves for two weeks of extremely hot weather.

If UCT is not a proper indicator for how an individual or population will react to rising temperatures, we must find another metric to better reflect thermal limitations. Mitchell et al. (2018) has proposed three new “zones” that better represent physiologically relevant temperature ranges: the “prescriptive zone”, the “tolerance zone”, and the “survival zone”. The “prescriptive zone” is wider than the traditional TNZ and refers to the temperature range over which body temperature varies with metabolic rate and activity level but not ambient heat load (Mitchell et al., 2018). Wider still is the “tolerance zone” where a stable body temperature is no longer maintained, and an endotherm may exhibit hypo- or hyperthermia (Mitchell et al., 2018). The “survival zone” is the widest range in which individuals are at risk of death via heat stroke or cold injury (Mitchell et al., 2018). Zone limits will vary based on the magnitude and duration of heat exposure, but Mitchell et al. (2018) offers a new approach for evaluating temperature’s effect on endotherm thermoregulation.

To complement the results of my respirometry experiment and UCT findings, I used free-ranging body temperature to explore the possibility of heterothermy as another thermoregulatory strategy used by flying squirrels. Core body temperature of *G. volans* has been measured once before using a captive population. Refinetti (1999) implanted three flying squirrels with radio sensor-transmitters to monitor the synchronicity of body temperature and locomotor activity. Squirrels were kept at 24°C in laboratory cages and exposed to a fixed photo period of 14L:10D. Body temperature and activity were recorded every 6 minutes for 1 week. Average body temperature ranged between 36-38°C with higher temperatures occurring during the nocturnal activity period. Locomotor activity and body temperature were highly synchronized when compared to other species in the study.

In agreement with Refinetti (1999), I found that southern flying squirrels have a higher body temperature (T_b) at night during their active phase and lower T_b during the day when resting ($\Delta T_b = \sim 2^\circ\text{C}$; Figure 8). The daily rhythmicity in T_b closely matched photoperiod but was independent of ambient temperature (Figures 6-7). A “circadian pacemaker” may control the daily rhythmicity of body temperature, but it likely does not control the fine-tune adjustments used for thermoregulation during the resting or active phase (Refinetti, 1999). To better understand finer scale T_b variability, I used the Heterothermy Index (Boyles et al., 2010).

The standardized Heterothermy Index allows for comparison of T_b variability between individuals and against other species for which an HI value exists. The all-squirrel, average HI value calculated from my data is 1.93 (Table 3). An HI value of 1.93 is close to those calculated for two other members of the squirrel family during the summer, *Spermophilus perryi* (HI = 1.43) and *Xerus inauris* (HI = 1.89) and greater than all other rodents with a published HI (minimum HI = 0.70, maximum HI = 1.36; Boyles et al., 2013).

The Arctic ground squirrel, *S. perryi*, and the Cape ground squirrel, *X. inauris*, differ considerably from flying squirrels in some key respects. Both of these species are diurnal, ground-dwelling squirrels that live in extreme environments (Skurski and Waterman, 2005; McLean, 2018). The Arctic ground squirrel inhabits northern Canada, Alaska, and parts of Siberia located within the Arctic Circle where it is a seasonal hibernator, frequently studied for its unique thermoregulatory behaviors (McLean, 2018). The Cape ground squirrel occupies arid environments in southern Africa (Skurski and Waterman, 2005). It does not hibernate, but it digs underground burrows for thermal refugia and uses its parasol-like tail to provide shade while foraging (Skurski and Waterman, 2005).

Southern flying squirrels inhabit much milder climates than either *S. perryii* or *X. inauris* but show a higher level of heterothermy as measured by HI. Similar HI values could represent an inherent thermoregulatory trait present in all squirrels that defines similar levels of heterothermy despite environmental variation. In contrast, the difference in HI values between *G. volans* and either *S. perryii* or *X. inauris* could be ecologically relevant. The vastly different methods of locomotion (gliding versus walking) and their associated morphologies could support different thermoregulatory strategies (daily heterothermy versus hibernation versus elevated RMR). Regardless, the Heterothermy Index is still quite new and must be calculated for more squirrel species before any definitive comparisons can be made.

The apparent variation in the body temperature of southern flying squirrels was driven, in part, by ambient temperature but not to the degree I had anticipated (see Appendix 3). I suspect that my measurement of ambient temperature did not match that experienced by flying squirrels, which subsequently led to some error in my models. Flying squirrels, like other small mammals, inhabit their own microclimate which may greatly differ from the average forest temperature (Varner and Dearing, 2014). Flying squirrels construct nests in tree hollows or on the forest floor using various plant fibers, but the insulative effect of nests has been studied primarily in cold weather not in heat (Stains, 1961; Muul, 1968; Muul, 1974; Isaac et al., 2008; Trudeau et al., 2011). In the winter, tree hollow nests sustain warmer temperatures and reduced variability, resulting in energy savings for flying squirrels (Muul, 1968). Similarly, Stains (1961) monitored temperature inside and outside of raccoon-inhabited (*Procyon lotor*) tree cavities year-round and found less variability inside tree cavities than outside but little difference in average hourly temperature between the two. Isaac et al. (2008) studied geometrically similar occupied and unoccupied tree cavities in northern Australia to detect thermal preferences in the den sites of the

common brushtail possum (*Trichosurus vulpecula*). Occupied cavities were 1.6°C cooler, had less temperature variability, and had lower extremes than unoccupied cavities (Isaac et al., 2008).

Whether or not flying squirrels are reaping thermal benefits from nest sites in the summer is currently unknown. The research of Stains (1961) and Isaac et al. (2008) suggests that nest temperature should be less variable than overall forest temperature and that cooler hollows may be preferred. However, without direct measurements of nest temperature and occupancy, it is impossible to assert that nest sites confer a thermal benefit in summer. The insulative effect could even trap body heat and elevate the nest temperature over that of the forest.

Furthermore, the insulative properties of the nest itself are not the only factors determining the microclimate for a flying squirrel. Group nesting is well documented in all species of North American flying squirrel (Dolan and Carter, 1977; Wells-Gosling and Heaney, 1984). Group nesting is primarily used to maintain warmth in the winter and reduce the energy required for thermoregulation; however, flying squirrel aggregations are found year-round throughout the geographic range of *G. volans* and *G. sabrinus* (Muul, 1974; Stapp et al., 1991; Layne and Raymond, 1994). Because of its pervasiveness across time and space, group nesting must provide additional benefits beyond thermoregulation that are most likely social (Muul, 1974; Stapp et al., 1991; Layne and Raymond, 1994).

Large aggregations of flying squirrels increase temperature within a nest through thermoregulation, increase insulation of the nest with additional pelage, and decrease heat loss by decreasing the surface area to volume ratio (Muul, 1968). Despite being a benefit in the winter, group nesting could be a detriment as temperatures rise (Muul, 1974). Temperatures of group nests could get too warm, forcing flying squirrel to change behavior. Such changes could include increased use of cooling mechanisms via higher energy expenditure, solitary nesting, or

producing smaller litters to reduce maternal heat loads. Regardless of the coping mechanism, flying squirrels will need to find some way to remedy the high heat load generated from their current nesting behaviors.

3.5 Conclusions

Southern flying squirrels do not significantly increase their resting metabolic rate with increasing ambient temperature, but they do show an increase in evaporative water loss and body temperature. Although they will not have to alter energy budgets to keep up with an increasing metabolic rate, flying squirrels will be forced to make behavioral changes as temperatures rise. Evaporative water loss is an effective cooling strategy so long as water supply is adequate (Mitchell et al., 2018). Flying squirrels may have to increase their water intake to compensate for the amount used during evaporative cooling when temperatures are above 36.2°C. Access to water should not be an issue in the forest habitat of *G. volans*, but any increase in resource demand may require allocation of energy.

Incidence and degree of heterothermy may also change as ambient temperatures increase. The free-ranging body temperature experiment revealed a level of heterothermy on par with other squirrel species, including one living in a hot, arid environment. The experimental period was too short, however, to reveal any seasonal changes and did not provide an indication of any costs that may be associated with the observed level of heterothermy. More research on the seasonality of and constraints to heterothermy needs to be conducted to better understand how this thermal strategy fits into the ecology of *G. volans*.

Furthermore, additional research on the microclimate experienced by flying squirrels is crucial for the improved understanding of this study's results and for the accurate prediction of future changes to Maine's *G. volans* population. How nest sites and aggregations will change as

temperatures rise is yet to be determined but will certainly influence the ecology and further expansion of southern flying squirrels.

G. volans' reaction to high temperatures throughout the experiments brings us back to my original question: what will happen to *G. sabrinus*? Northern flying squirrels may show a marked increase in resting metabolic rate as temperatures rise or initiate evaporative cooling at a lower ambient temperature. Perhaps, they exhibit less body temperature variation and would generate an HI value closer to that of the Arctic ground squirrel. Maybe, *G. sabrinus* shows a similar response to high temperatures as *G. volans* and the observed range shifts have nothing to do with thermal tolerance. My research does not reveal the answers to these questions, but it does provide a basis for future comparison and is one of the first investigations into the relationship between global climate warming and flying squirrel ecophysiology.

REFERENCES

- Araújo, M. B. and Peterson, A. T.** (2012). Uses and misuses of bioclimatic envelope modeling. *Ecology* **93**, 1527–1539.
- Arbogast, B. S., Schumacher, K. I., Kerhoulas, N. J., Bidlack, A. L., Cook, J. A. and Kenagy, G. J.** (2017). Genetic data reveal a cryptic species of New World flying squirrel: *Glaucomys oregonensis*. *Journal of Mammalogy* **98**, 1027–1041.
- Bivand, R. and Lewin-Koh, N.** (2018). maptools: Tools for Handling Spatial Objects. R package version 0.9-4. <https://CRAN.R-project.org/package=maptools>.
- Bowman, J., Holloway, G. L., Malcolm, J. R., Middel, K. R. and Wilson, P. J.** (2005). Northern range boundary dynamics of southern flying squirrels: evidence of an energetic bottleneck. *Canadian Journal of Zoology* **83**, 1486–1494.
- Boyles, J. G., Smit, B. and McKechnie, A. E.** (2011). A New Comparative Metric for Estimating Heterothermy in Endotherms. *Physiological and Biochemical Zoology* **84**, 115–123.
- Boyles, J. G., Thompson, A. B., McKechnie, A. E., Malan, E., Humphries, M. M. and Careau, V.** (2013). A global heterothermic continuum in mammals: Global patterns of heterothermy in mammals. *Global Ecology and Biogeography* **22**, 1029–1039.
- Buckley, L. B.** (2008). Linking Traits to Energetics and Population Dynamics to Predict Lizard Ranges in Changing Environments. *The American Naturalist* **171**, E1–E19.
- Cassola, F.** (2016). *Glaucomys volans*. *The IUCN Red List of Threatened Species 2016*: e.T9240A115091392. <http://dx.doi.org/10.2305/IUCN.UK.2016-3.RLTS.T9240A22257175.en>.
- Cassola, F.** (2016). *Glaucomys sabrinus*. *The IUCN Red List of Threatened Species 2016*: e.T39553A22256914. <http://dx.doi.org/10.2305/IUCN.UK.2016-3.RLTS.T39553A22256914.en>.
- Chappell, M. A. and Bartholomew, G. A.** (1981). Activity and Thermoregulation of the Antelope Ground Squirrel *Ammospermophilus leucurus* in Winter and Summer. *Physiological Zoology* **54**, 215–223.
- Dolan, P. G. and Carter, D. C.** (1977). *Glaucomys volans*. *Mammalian Species* **1**.
- Fernandez, I.J., C.V. Schmitt, S.D. Birkel, E. Stancioff, A.J. Pershing, J.T. Kelley, J.A. Runge, G.L. Jacobson, and P.A. Mayewski.** (2015). *Maine's Climate Future: 2015 Update*. Orono, ME: University of Maine.

- Fridell, R. A. and Litvaitis, J. A.** (1991). Influence of resource distribution and abundance on home-range characteristics of southern flying squirrels. *Canadian Journal of Zoology* **69**, 2589–2593.
- Garroway, C. J., Bowman, J., Cascaden, T. J., Holloway, G. L., Mahan, C. G., Malcolm, J. R., Steele, M. A., Turner, G. and Wilson, P. J.** (2010). Climate change induced hybridization in flying squirrels. *Global Change Biology* **16**, 113–121.
- Garroway, C. J., Bowman, J., Holloway, G. L., Malcolm, J. R. and Wilson, P. J.** (2011). The genetic signature of rapid range expansion by flying squirrels in response to contemporary climate warming. *Global Change Biology* **17**, 1760–1769.
- Hobbs, R. J., Higgs, E. and Harris, J. A.** (2009). Novel ecosystems: implications for conservation and restoration. *Trends in Ecology & Evolution* **24**, 599–605.
- Huey, R. B., Kearney, M. R., Krockenberger, A., Holtum, J. A. M., Jess, M. and Williams, S. E.** (2012). Predicting organismal vulnerability to climate warming: roles of behaviour, physiology and adaptation. *Philosophical Transactions of the Royal Society B: Biological Sciences* **367**, 1665–1679.
- Humphries, M. M.** (2004). Bioenergetic Prediction of Climate Change Impacts on Northern Mammals. *Integrative and Comparative Biology* **44**, 152–162.
- IPCC.** (2014). *Climate Change 2014: Synthesis Report*. Fifth Assessment Report of the Intergovernmental Panel on Climate Change.
- Isaac, J. L., De Gabriel, J. L. and Goodman, B. A.** (2008). Microclimate of daytime den sites in a tropical possum: implications for the conservation of tropical arboreal marsupials. *Animal Conservation* **11**, 281–287.
- Kearney, M. and Porter, W.** (2009). Mechanistic niche modelling: combining physiological and spatial data to predict species' ranges. *Ecology Letters* **12**, 334–350.
- Larivée, M. L., Boutin, S., Speakman, J. R., McAdam, A. G. and Humphries, M. M.** (2010). Associations between over-winter survival and resting metabolic rate in juvenile North American red squirrels: *Resting metabolic rate and survival*. *Functional Ecology* **24**, 597–607.
- Levesque, D. L., Nowack, J. and Stawski, C.** (2016). Modelling mammalian energetics: the heterothermy problem. *Climate Change Responses* **3**,.
- Levesque, D. L., Menzies, A. K., Landry-Cuerrier, M., Larocque, G. and Humphries, M. M.** (2017). Embracing heterothermic diversity: non-stationary waveform analysis of temperature variation in endotherms. *Journal of Comparative Physiology B* **187**, 749–757.

- Lighton, J. R. B.** (2008). *Measuring metabolic rates: a manual for scientists*. Oxford ; New York: Oxford University Press.
- Maser, C., Trappe, J. M. and Nussbaum, R. A.** (1978). Fungal-Small Mammal Interrelationships with Emphasis on Oregon Coniferous Forests. *Ecology* **59**, 799–809.
- Maser, C., Maser, Z., Witt, J. W. and Hunt, G.** (1986). The northern flying squirrel: a mycophagist in southwestern Oregon. *Canadian Journal of Zoology* **64**, 2086–2089.
- Mazerolle, M. J.** (2017). AICcmodavg: Model selection and multimodel inference based on (Q)AIC(c). R package version 2.1-1. <https://cran.r-project.org/package=AICcmodavg>.
- McKechnie, A. E., Smit, B., Whitfield, M. C., Noakes, M. J., Talbot, W. A., Garcia, M., Gerson, A. R. and Wolf, B. O.** (2016). Avian thermoregulation in the heat: evaporative cooling capacity in an archetypal desert specialist, Burchell's sandgrouse (*Pterocles burchelli*). *The Journal of Experimental Biology* **219**, 2137–2144.
- McLean, B. S.** (2018). *Urocitellus parryii* (Rodentia: Sciuridae). *Mammalian Species* **50**, 84–99.
- Merritt, J. F., Zegers, D. A. and Rose, L. R.** (2001). Seasonal thermogenesis of southern flying squirrels (*Glaucomys volans*). *Journal of Mammalogy* **82**, 51–64.
- Mitchell, D., Snelling, E. P., Hetem, R. S., Maloney, S. K., Strauss, W. M. and Fuller, A.** (2018). Revisiting concepts of thermal physiology: Predicting responses of mammals to climate change. *Journal of Animal Ecology* **87**, 956–973.
- Mole, M. A., Rodrigues DÁraujo, S., van Aarde, R. J., Mitchell, D. and Fuller, A.** (2016). Coping with heat: behavioural and physiological responses of savanna elephants in their natural habitat. *Conservation Physiology* **4**, cow044.
- Muggeo, V. M. R.** (2008). segmented: an R Package to Fit Regression Models with Broken-Line Relationships. R News, 8/1, 20-25. URL <https://cran.r-project.org/doc/Rnews/>.
- Muul, I.** (1974). Geographic Variation in the Nesting Habits of *Glaucomys volans*. *Journal of Mammalogy* **55**, 840–844.
- Myers, P., Lundrigan, B. L., Hoffman, S. M. G., Haraminac, A. P. and Seto, S. H.** (2009). Climate-induced changes in the small mammal communities of the Northern Great Lakes Region. *Global Change Biology* **15**, 1434–1454.
- Neumann, R. L.** (1967). Metabolism in the eastern chipmunk (*Tamias striatus*) and the southern flying squirrel (*Glaucomys volans*) during the winter and summer. *Proceedings of the Third International Symposium on Natural Mammalian Hibernation*.
- Olson, M. N., Bowman, J. and Burness, G.** (2017). Seasonal energetics and torpor use in North American flying squirrels. *Journal of Thermal Biology* **70**, 46–53.

- Parmesan, C.** (2006). Ecological and Evolutionary Responses to Recent Climate Change. *Annual Review of Ecology, Evolution, and Systematics* **37**, 637–669.
- Pauli, J. N., Dubay, S. A., Anderson, E. M. and Taft, S. J.** (2004). Strongyloides robustus and the Northern Sympatric Populations of Northern (*Glaucomys sabrinus*) and Southern (*G. volans*) Flying Squirrels. *Journal of Wildlife Diseases* **40**, 579–582.
- Pinheiro J, Bates D, DebRoy S, Sarkar D, R Core Team.** (2018). nlme: Linear and Nonlinear Mixed Effects Models. R package version 3.1-137, <https://CRAN.R-project.org/package=nlme>.
- Porter, W. P. and Gates, D. M.** (1969). Thermodynamic Equilibria of Animals with Environment. *Ecological Monographs* **39**, 227–244.
- R Core Team.** (2016). R: A language and environment for statistical computing. R Foundation for Statistical Computing, Vienna, Austria. <https://www.R-project.org/>
- Refinetti, R.** (1999). Relationship between the daily rhythms of locomotor activity and body temperature in eight mammalian species. *American Journal of Physiology* **277**, R1493–R1500.
- Ruben, J.** (1995). The Evolution of Endothermy in Mammals and Birds: From Physiology to Fossils. *Annual Review of Physiology* **57**, 69–95.
- Scholander, P. F.** (1955). Evolution of Climatic Adaptation in Homeotherms. *Evolution* **9**, 15.
- Scholander, P. F., Hock, R., Walters, V., Johnson, F. and Irving, L.** (1950). HEAT REGULATION IN SOME ARCTIC AND TROPICAL MAMMALS AND BIRDS. *The Biological Bulletin* **99**, 237–258.
- Schulte-Hostedde, A. I., Millar, J. S. and Hickling, G. J.** (2001). Evaluating body condition in small mammals. *Canadian Journal of Zoology* **79**, 1021–1029.
- Seebacher, F. and Franklin, C. E.** (2012). Determining environmental causes of biological effects: the need for a mechanistic physiological dimension in conservation biology. *Philosophical Transactions of the Royal Society B: Biological Sciences* **367**, 1607–1614.
- Skurski, D. A. and Waterman, J. M.** (2005). *Xerus inauris*. *Mammalian Species* **781**, 1–4.
- Smith, W. P.** (2007). Ecology of *Glaucomys sabrinus*: Habitat, Demography, and Community Relations. *Journal of Mammalogy* **88**, 862–881.
- Stapp, P.** (1992). Energetic Influences on the Life History of *Glaucomys volans*. *Journal of Mammalogy* **73**, 914–920.

- Stapp, P., Pekins, P. J. and Mautz, W. W.** (1991). Winter energy expenditure and the distribution of southern flying squirrels. *Canadian Journal of Zoology* **69**, 2548–2555.
- Steele, M. A. and Koprowski, J. L.** (2001). *North American tree squirrels*. Washington: Smithsonian Institution Press.
- Thorington, R. W. ed.** (2012). *Squirrels of the world*. Baltimore: Johns Hopkins University Press.
- Varner, J. and Dearing, M. D.** (2014). The Importance of Biologically Relevant Microclimates in Habitat Suitability Assessments. *PLoS ONE* **9**, e104648.
- Weigl, P. D.** (1978). Resource Overlap, Interspecific Interactions and the Distribution of the Flying Squirrels, *Glaucomys volans* and *G. sabrinus*. *American Midland Naturalist* **100**, 83.
- Wells-Gosling, N. and Heaney, L. R.** (1984). *Glaucomys sabrinus*. *Mammalian Species* **1**.
- Wells-Gosling, N.** (1985). *Flying squirrels: gliders in the dark*. 1st ed. Washington, D.C: Smithsonian Institution Press.
- Wetzel, E. J. and Weigl, P. D.** (1994). Ecological implications for flying squirrels (*Glaucomys* spp.) of effects of temperature on the in vitro development and behavior of *strongyloides robustus*. *American Midland Naturalist* **131**, 43–54.
- White, C. R. and Seymour, R. S.** (2004). Does Basal Metabolic Rate Contain a Useful Signal? Mammalian BMR Allometry and Correlations with a Selection of Physiological, Ecological, and Life-History Variables. *Physiological and Biochemical Zoology* **77**, 929–941.
- Whitfield, M. C., Smit, B., McKechnie, A. E. and Wolf, B. O.** (2015). Avian thermoregulation in the heat: scaling of heat tolerance and evaporative cooling capacity in three southern African arid-zone passerines. *Journal of Experimental Biology* **218**, 1705–1714.
- Wickham, H.** (2011). The Split-Apply-Combine Strategy for Data Analysis. *Journal of Statistical Software*, 40(1), 1-29. <http://www.jstatsoft.org/v40/i01/>.
- Wickham, H.** (2016). *ggplot2: Elegant Graphics for Data Analysis*. New York: Springer-Verlag.
- Wilke, C. O.** (2018). cowplot: Streamlined Plot Theme and Plot Annotations for 'ggplot2'. R package version 0.9.3. <https://CRAN.R-project.org/package=cowplot>
- Withers, P. C.** (1992). *Comparative animal physiology*. Fort Worth: Saunders College Pub.

Withers, P. C. (2001). Design, calibration and calculation for flow-through respirometry systems. *Australian Journal of Zoology* **49**, 445–461.

Withers, P. C., Cooper, C. E., Maloney, S. K., Bozinovic, F. and Cruz Neto, A. P. (2016). *Ecological and Environmental Physiology of Mammals*. Oxford University Press.

Wood, C. M., Witham, J. W. and Hunter, M. L. (2016). Climate-driven range shifts are stochastic processes at a local level: two flying squirrel species in Maine. *Ecosphere* **7**,.

APPENDIX 1

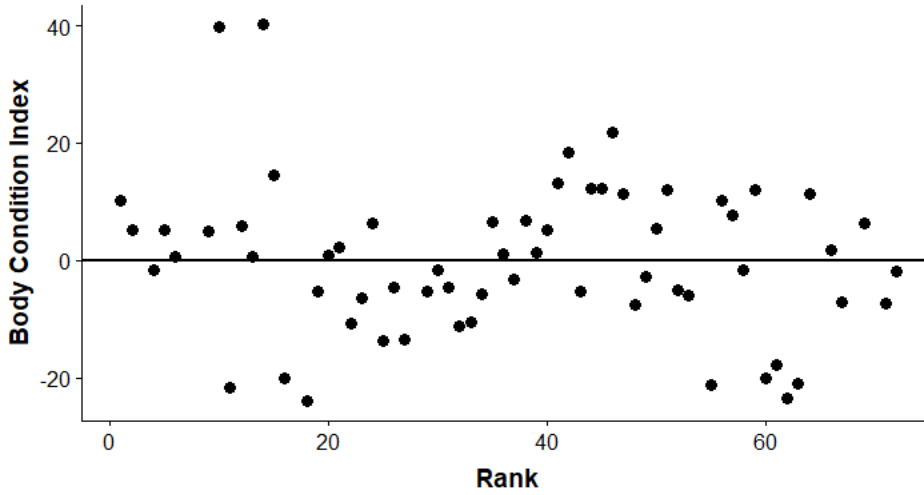


Figure 9: Body Condition Index (BCI) for *G. volans* from 2017-2018. BCI is the residual calculated from regressing body weight on forearm length as seen in Schulte-Hostedde et al., 2001. Positive numbers indicate healthier, fatter individuals and negative numbers indicate less healthy, leaner individuals.

APPENDIX 1 CONT.

Table 4: Morphometric measurements for captured *G. volans* from 2017-2018. Only records from first capture of the year are included. * indicate questionable sex identification.

ID	Date	Sex	Weight (g)	Forearm (mm)	Hindfoot w/o Toes (mm)	Hindfoot w/ Toes (mm)	Ear (mm)	Body Condition Index
UM001	05/16/2017	F	70	24	15	-	16	10.08
UM002	05/21/2017	F	62.3	18	18.19	28.01	8	5.17
UM003	05/21/2017	M	-	17	13	-	11	-
UM005	05/24/2017	F	62	32	21.5	27.5	14	-1.64
UM006	05/28/2017	M	63.7	21	21	-	5	5.18
UM007	05/29/2017	M	65	33.46	18.93	27	11.15	0.68
UM008	05/29/2017	M	61.3	-	16	24	-	-
UM000	06/02/2017	M	-	21	15	21	-	-
UM009	06/14/2017	M	63	20	-	-	13.01	4.94
UM010	06/14/2017	F	101	26.73	17.2	25.4	9.4	39.81
UM011	06/14/2017	M	35	17	-	29.22	14.9	-21.66
UM012	06/15/2017	M	67	26.44	22.9	26.84	12.34	5.95
UM013	06/15/2017	M	61	24.9	-	26.9	15.7	0.66
UM797	06/28/2017	F	101	25.8	-	31.96	-	40.25
UM757	06/28/2017	F	76	27.6	-	29.5	-	14.41
UM792	06/29/2017	M	38	20.17	-	20.7	11.5	-20.14
UM805	06/29/2017	M	18.8	-	-	27.7	-	-
UM014	07/24/2017	F*	38	28.62	17.74	27.15	13.63	-24.07
UM015	07/24/2017	M	55	25	15	22	8	-5.38
UM037	07/26/2017	F	64	30.96	20.01	28.62	13.19	0.85
UM016	07/26/2017	F	65	29.98	20.24	28.43	11.21	2.30
UM017	07/26/2017	F	53	32.03	22.5	30.05	12.88	-10.65
UM020	08/01/2017	F	58	33.9	19.17	28.84	10.49	-6.52
UM021	08/01/2017	F	71	34.44	23.43	29.06	11.92	6.23
UM026	08/01/2017	M	49	29.98	19.82	28.14	11.93	-13.70
UM027	08/02/2017	M	61	36.46	21.03	25.95	10.43	-4.71
UM028	08/02/2017	F	52	35.91	21.72	27.51	10.29	-13.45

APPENDIX 1 CONT.

Table 4 Cont.

ID	Date	Sex	Weight (g)	Forearm (mm)	Hindfoot w/o Toes (mm)	Hindfoot w/ Toes (mm)	Ear (mm)	Body Condition Index
UM030	08/03/2017	F	67	-	-	-	-	-
UM031	08/04/2017	M*	60	35.38	19.11	27.79	10.42	-5.21
UM032	08/04/2017	F	64	36.27	21.36	26.49	10.56	-1.62
UM033	08/25/2017	F	59	31.93	20.47	22.21	11.26	-4.60
UM798	08/26/2017	F	53	33.07	19.5	26.39	9.69	-11.13
UM034	09/01/2017	F	52	29.76	18.27	27.44	14.6	-10.60
UM999	09/01/2017	M	60	36.55	19.91	28.74	16.09	-5.75
UM075	11/12/2017	F	71	34	25	31	14	6.43
UM804	11/14/2017	M	66	35	22	29.5	14	0.97
UM399	05/06/2018	F	61	33.5	19.5	28	8	-3.33
UM400	05/06/2018	M	70	31	24	29	13	6.82
UM073	05/08/2018	M	63	28	17	24	7	1.22
UM726	05/08/2018	M	66	26	17	20	8	5.15
UM381	05/10/2018	M	74	26	13	21	7	13.15
UM072	05/10/2018	F	81	30	16	23	10	18.29
UM051	05/25/2018	M	56	27	16	22	10	-5.31
UM787	05/25/2018	F	73	26	16	24	8	12.15
UM037	05/25/2018	F	73	26	16	24	8	12.15
UM795	05/26/2018	F	84	29	17	22	8	21.76
UM698	05/27/2018	F	74	30	16	24	8	11.29
UM071	05/30/2018	F	56	32	14	21	5	-7.64
UM070	05/30/2018	F	59	28	17	21	10	-2.78
UM076	06/09/2018	M	65.8	25	16	22	10	5.41
UM075	06/10/2018	F	73.7	28	17	22	8	11.92
UM052	06/11/2018	F	55.3	25	16	20	11	-5.08
UM796	06/21/2018	M*	54.3	25	15	19	6	-6.08
UM012	06/21/2018	F	65.9	-	-	-	-	-

APPENDIX 1 CONT.

Table 4 Cont.

ID	Date	Sex	Weight (g)	Forearm (mm)	Hindfoot w/o Toes (mm)	Hindfoot w/ Toes (mm)	Ear (mm)	Body Condition Index
UM686	06/22/2018	F	38.8	24	18	26	11	-21.12
UM738	06/22/2018	F	73.3	31	18	23	8	10.13
UM802	06/22/2018	M	70.9	31	17	22	9	7.73
UM749	06/22/2018	F	59.6	27	16	24	-	-1.71
UM679	06/22/2018	F*	76.5	34	17	23	-	11.93
UM716	06/23/2018	F	40.8	26	14	25	9	-20.05
UM773	06/23/2018	M	41.7	23	14	24	9	-17.75
UM555	06/30/2018	F	39.2	30	16	21	10	-23.51
UM808	06/30/2018	M	39.9	26	15	24	7	-20.95
UM718	07/03/2018	F	73.1	28	19	24	7	11.32
UM053	07/03/2018	M	66.6	-	-	-	-	-
UM799	07/30/2018	F	63.5	28	16	24	6	1.72
UM742	08/02/2018	F	54.6	28	17	23	7	-7.18
UM740	08/02/2018	M	-	29	19	23	11	-
UM812	08/11/2018	F*	66.7	25	13	20	8	6.32
UM781	08/11/2018	M	63.1	-	13	21	6	-
UM731	08/12/2018	M	55.9	31	15	24	6	-7.27
UM780	08/21/2018	F*	59.5	27	14	21	7	-1.81

APPENDIX 2

Table 5: Respirometry models. Ranking was performed using corrected Akaike Information Criterion (AIC_c) scores and Akaike weights (AIC_cWt). All models with an AIC_cWt>0 are presented and the number of parameters contained in the model are included (k).

Model Parameters	k	AIC _c	AIC _c Wt
RMR^b			
'T _a ' + 'StartMass'	5	494.50	0.42
'T _a ' * 'StartMass'	6	495.55	0.25
'T _a ' + 'StartMass' + 'Sex'	6	496.59	0.15
'T _a ' * 'StartMass' + 'Sex'	7	497.79	0.08
'T _a ' + 'StartMass' * 'Sex'	7	499.01	0.04
'T _a '	4	500.21	0.02
'T _a ' + 'Sex'	5	501.19	0.01
'T _a ' * 'Sex'	6	503.18	0.01
EWL^a			
'T _a ' * 'StartMass'	5	695.34	0.65
'T _a ' * 'StartMass' + 'Sex'	6	697.87	0.18
'T _a '	3	699.81	0.07
'T _a ' + 'StartMass'	4	701.36	0.03
'T _a ' + 'Sex'	4	701.58	0.03
'T _a ' * 'Sex'	5	702.25	0.02
'T _a ' + 'StartMass' + 'Sex'	5	703.70	0.01
'T _a ' * 'StartMass' * 'Sex'	9	704.23	0.01
T_{sub}^b			
'T _a ' + 'StartMass'	5	127.50	0.45
'T _a ' + 'StartMass' + 'Sex'	6	129.11	0.20
'T _a ' * 'StartMass'	6	129.21	0.19
'T _a ' * 'StartMass' + 'Sex'	7	130.90	0.08
'T _a ' + 'StartMass' * 'Sex'	7	131.45	0.06
MHP/EHL^a			
'T _a '	3	-52.30	0.32
'T _a ' * 'StartMass'	5	-51.95	0.27
'T _a ' + 'Sex'	4	-50.17	0.11
'T _a ' + 'StartMass'	4	-50.05	0.10
'T _a ' * 'StartMass' + 'Sex'	6	-49.76	0.09
'T _a ' * 'Sex'	5	-48.73	0.05
'T _a ' + 'StartMass' + 'Sex'	5	-48.21	0.04
'T _a ' + 'StartMass' * 'Sex'	6	-45.69	0.01

^aVariance structure used: weights = varFixed(~Ta), ^bVariance structure used: weights = varIdent(form=~1|Sex)

APPENDIX 3: BODY TEMPERATURE MODELS

Table 6: Core body temperature models. Ranking was performed using corrected Akaike Information Criterion (AIC_c) scores and Akaike weights (AIC_cWt). All models with an AIC_cWt>0 are presented and the number of parameters contained in the model are included (k).

Model Parameters ^{a,b}	k	AIC _c	AIC _c Wt
T_{bmax}			
'Date'	5	-133.13	0.5
'Date' + 'MaxT _b '	6	-132.50	0.37
'Date' * 'MaxT _b '	7	-130.43	0.13
'MaxT _b '	5	-118.30	0.00
T_{bmin}			
'Date' * 'MinT _b '	7	211.02	0.72
'Date' + 'MinT _b '	6	212.90	0.28
'MinT _b '	5	221.16	0.00
'Date'	5	242.20	0.00
T_{bdelta}			
'Date'	7	309.66	0.49
'Date' + 'deltaT _b '	8	311.09	0.24
'deltaT _b '	7	311.97	0.15
'Date' * 'deltaT _b '	9	312.39	0.12

^aAll models were corrected for autocorrelation using the correlation structure corCAR1 (form = ~1|Animal ID, ^b~1|Animal ID was used as a random factor

BIBLIOGRAPHY OF THE AUTHOR

Vanessa Hensley was born in Cedar Falls, Iowa on November 21, 1990. She was raised in Cedar Falls, Iowa and graduated from Cedar Falls High School in 2009. She attended Washington University in St. Louis and graduated in 2013 with a Bachelor's degree in Environmental Studies and Spanish. She worked as an Aquarium Biologist at Mote Marine Laboratory and Aquarium from 2014-2016 when she first encountered thermal physiology and metabolic rate research. She entered the Ecology and Environmental Sciences graduate program at the University of Maine in the fall of 2016 to work with Dr. Danielle Levesque on the ecophysiology of flying squirrels. After receiving her degree, Vanessa will be searching for work in Minnesota. Vanessa is a candidate for the Master of Science degree in Ecology and Environmental Sciences from the University of Maine in May 2019.